

A graph-based approach for the approximate solution of the chemical master equation

Raffaele Basile

Ramon Grima

Nikola Popović

February 17, 2015

Abstract

The chemical master equation (CME) represents the accepted stochastic description of chemical reaction kinetics in mesoscopic systems. As its exact solution – which gives the corresponding probability density function – is possible only in very simple cases, there is a clear need for approximation techniques. Here, we propose a novel perturbative three-step approach which draws heavily on graph theory: (i) we expand the eigenvalues of the transition state matrix in the CME as a series in a non-dimensional parameter that depends on the reaction rates and the reaction volume; (ii) we derive an analogous series for the corresponding eigenvectors via a graph-based algorithm; (iii) we combine the resulting expansions into an approximate solution to the CME. We illustrate our approach by applying it to a reversible dimerization reaction; then, we formulate a set of conditions which ensure its applicability to more general reaction networks, and we verify those conditions for two common catalytic mechanisms. Comparing our results with the linear-noise approximation (LNA), we find that our methodology is consistently more accurate for sufficiently small values of the non-dimensional parameter. This superior accuracy is particularly evident in scenarios characterized by small molecule numbers, which are typical of conditions inside biological cells.

1 Introduction

Chemical reaction kinetics have traditionally been modeled by means of rate equations. These are (sets of) deterministic ordinary differential equations that describe the time-evolution of the concentrations of chemical species; see, *e.g.*, [28] and the references therein. However, it is well known that chemical reaction kinetics are inherently stochastic [16]: while the dynamics average out and appear deterministic if the spatial scale is sufficiently large, on mesoscopic scales the probabilistic nature of reaction networks cannot be ignored [24]. Hence, rate equations are useful in the description of reaction kinetics in macroscopic volumes such as test tubes and large-size chemical reactors, but cannot accurately describe the kinetics in smaller volumes; a prominent example are biochemical reactions occurring inside biological cells [24].

The chemical master equation (CME) constitutes the accepted mesoscopic description of chemical reaction processes; it can be derived from combinatorial arguments [35] or from microscopic physics [15]. The derivation typically assumes well-mixed and dilute conditions, as in [15]; however, a modified version also exists for non-dilute regimes [19]. The CME contains information about the mean concentrations of reactants and the fluctuations about them at all points in time; mathematically, it is a set of linear differential equations for the probabilities of the states in the system. The typically large dimensionality of the state space implies that it is virtually impossible to find simple analytical expressions for the solution of the CME, *i.e.*, the probability density function of the underlying reaction network. Known cases in which the CME is solvable in closed form are few, and include systems that are composed purely of first-order non-catalytic reactions [12, 13, 26], as well as a rudimentary genetic feedback loop [23]; however, the former are not typical of naturally occurring reaction networks. Hence, over the past few decades, a range of approximation techniques have been developed to investigate systems composed of both first-order and second-order (bimolecular) processes. Amongst these the most popular are the linear-noise (Gaussian) approximation (LNA) [35, 7] and moment-closure approximations [17, 10]. However, only the former technique provides a systematic approximation algorithm, whereas the latter is based on an ad-hoc truncation of the moment equations [22]. (An alternative approach, the so-called Poisson representation [14], transforms the CME into an equivalent Fokker-Planck equation (FPE); however,

the corresponding solution typically cannot be found in closed form, but also has to be approximated.) On the other hand, the principal disadvantage of LNA is that it gives results in the limit of large reaction volumes and, hence, that it is not well-suited to the investigation of reaction processes in small volumes [25, 18, 20].

In this article, we develop a novel approximation technique for the solution of the CME which is applicable both for very small and for very large reaction volumes, and which thus provides a new analytical tool for understanding mesoscopic reaction kinetics. In the interest of pedagogical clarity, the approach is first developed for a simple bimolecular reaction, and is later extended to more general reaction networks.

The article is organized as follows. In Section 2, we introduce the CME for a dimerization reaction, we reduce it to non-dimensional matrix form, and we approximate the eigenvalues of the transition state matrix in the CME by a series expansion in powers of a non-dimensional combination of the reaction rate constants and the reaction volume. In Section 3, we develop the main theoretical result of this article, a graph-based methodology for determining the adjoint matrix of any given square matrix. In Section 4, we revisit the dimerization reaction to find an expansion for the matrix of eigenvectors of the transition matrix, as well as for the corresponding inverse matrix, on the basis of the theory developed in Section 3. In Section 5, we combine the results of the preceding three sections to construct an approximate solution to the CME for dimerization. We also compare our theoretical results with “exact” solutions of that CME – *i.e.*, with solutions obtained by numerical integration – and with the LNA. In Section 6, we explore the applicability of our graph-based approach to more complex sets of chemical reactions. We then summarize and discuss our findings in Section 7. We conclude with a series of appendices: in Appendix A, we cite general eigenvector formulae to supplement those in Section 4; in Appendix B, we present a brief derivation of LNA in the context of dimerization; finally, in Appendix C, we verify the conditions formulated in Section 6 for two examples involving catalysis.

2 Dimerization

To illustrate the approach developed here, we consider the simplest reversible bimolecular reaction, namely dimerization, whereby a pair of monomer molecules (species A) react to form a single dimer molecule (species B); the latter can dissociate back into free monomers: $A + A \rightleftharpoons B$. Despite its simplicity, dimerization is a ubiquitous component in various intracellular reaction networks [27].

2.1 The CME

In the following, we will assume the dimerization reaction defined above to occur in a compartment of volume Ω , with no influx or efflux of particles. We will also enforce well-mixed conditions such that the state of the system at any point in time can simply be described by the number of molecules of species A and B . The CME is then a time-evolution equation for $\mathbb{P}(n_A, n_B, t)$, the probability that, at time t , the system contains n_A molecules of type A and n_B molecules of type B ; it can be derived via a simple probabilistic analysis: defining $W(n_A, n_B | n'_A, n'_B) \Delta t$ as the probability that the system evolves from a state (n'_A, n'_B) to a state (n_A, n_B) within a (short) time interval Δt , we find the gain-loss equation

$$\begin{aligned} \mathbb{P}(n_A, n_B, t + \Delta t) = & W(n_A, n_B | n_A + 2, n_B - 1) \mathbb{P}(n_A + 2, n_B - 1, t) \Delta t \\ & + W(n_A, n_B | n_A - 2, n_B + 1) \mathbb{P}(n_A - 2, n_B + 1, t) \Delta t \\ & + [1 - W(n_A - 2, n_B + 1 | n_A, n_B) - W(n_A + 2, n_B - 1 | n_A, n_B)] \mathbb{P}(n_A, n_B, t) \Delta t. \end{aligned} \quad (1)$$

In words, the above equation can be parsed as follows: (i) the first line in (1) represents the gain of state (n_A, n_B) from state $(n_A + 2, n_B - 1)$ due to a forward reaction – two molecules of A bind to form one of B – occurring during the time interval Δt ; (ii) the second line describes the gain of state (n_A, n_B) from state $(n_A - 2, n_B + 1)$ due to a reverse reaction (dissociation of B into two molecules of A) occurring within the time interval Δt ; and (iii) the third and fourth lines correspond to the case where the system is already in state (n_A, n_B) at time t and no (forward or reverse) reaction occurs in the time interval Δt .

The functions W in (1) can be determined from combinatorial arguments [35]; we quote them without derivation here. If we are in state (n_A, n_B) , the probability of a forward reaction occurring within the time interval Δt is given by $W(n_A + 2, n_B - 1 | n_A, n_B) \Delta t = \frac{k_1}{\Omega} n_A (n_A - 1) \Delta t$, where k_1 is the forward rate constant (with units of volume divided

by time). Similarly, if we are in state (n_A, n_B) , the probability of a reverse reaction occurring in the time interval Δt is given by $W(n_A + 2, n_B - 1 | n_A, n_B) \Delta t = k_2 n_B \Delta t$, where k_2 is the reverse rate constant, with units of inverse time. By analogous arguments, one obtains $W(n_A, n_B | n_A + 2, n_B - 1) \Delta t = \frac{k_1}{\Omega} (n_A + 2)(n_A + 1) \Delta t$ and $W(n_A, n_B | n_A - 2, n_B + 1) = k_2 (n_B + 1) \Delta t$. (Here, we note that the rate constants k_1 and k_2 are the same as those found in the conventional deterministic rate equations [28].)

Substituting the functions W from above into Eq. (1) and taking the limit of infinitesimally small Δt , we finally obtain the CME for reversible dimerization:

$$\begin{aligned} \frac{d}{dt} \mathbb{P}(n_A, n_B, t) &= \frac{k_1}{\Omega} (n_A + 2)(n_A + 1) \mathbb{P}(n_A + 2, n_B - 1, t) + k_2 (n_B + 1) \mathbb{P}(n_A - 2, n_B + 1, t) \\ &\quad - \frac{k_1}{\Omega} n_A (n_A - 1) \mathbb{P}(n_A, n_B, t) - k_2 n_B \mathbb{P}(n_A, n_B, t). \end{aligned} \quad (2)$$

2.2 Non-dimensionalization and reduction

The dimerization reaction introduced above possesses a simple conservation law, namely, the total number of monomers (in free and bound form) is constant for all times: $n_{\text{tot}} := n_A + 2n_B$. In particular, the number of molecules of B can be expressed in terms of A , as $n_B = \frac{n_{\text{tot}}}{2} - \frac{n_A}{2}$. Thus, the possible states which can be accessed by the system are

$$n_A = \begin{cases} 1, 3, \dots, n_{\text{tot}} - 2, n_{\text{tot}} & \text{if } n_{\text{tot}} \text{ is odd,} \\ 0, 2, \dots, n_{\text{tot}} - 2, n_{\text{tot}} & \text{if } n_{\text{tot}} \text{ is even.} \end{cases}$$

For the following analysis, we may restrict ourselves to the case where n_{tot} is even, as the odd case can be treated in an analogous fashion. Moreover, we introduce the new constant α via $n_{\text{tot}} = 2\Omega\alpha$, where α represents half the maximum concentration of monomers in the reaction volume Ω . It follows that $n_B = \Omega\alpha - \frac{n_A}{2}$ and, hence, that the CME, Eq. (2), can be reduced to univariate form:

$$\begin{aligned} \frac{d}{dt} \mathbb{P}(n_A, t) &= \frac{k_1}{\Omega} (n_A + 2)(n_A + 1) \mathbb{P}(n_A + 2, t) + k_2 \left(\Omega\alpha - \frac{n_A}{2} + 1 \right) \mathbb{P}(n_A - 2, t) \\ &\quad - \frac{k_1}{\Omega} n_A (n_A - 1) \mathbb{P}(n_A, t) - k_2 \left(\Omega\alpha - \frac{n_A}{2} \right) \mathbb{P}(n_A, t). \end{aligned} \quad (3)$$

Next, we non-dimensionalize Eq. (3) by dividing the equation by k_2 and by rescaling the time variable, with $t \rightarrow k_2 t$, to obtain

$$\begin{aligned} \frac{d}{dt} \mathbb{P}(n_A, t) &= K (n_A + 2)(n_A + 1) \mathbb{P}(n_A + 2, t) + \left(\Omega\alpha - \frac{n_A}{2} + 1 \right) \mathbb{P}(n_A - 2, t) \\ &\quad - K n_A (n_A - 1) \mathbb{P}(n_A, t) - \left(\Omega\alpha - \frac{n_A}{2} \right) \mathbb{P}(n_A, t). \end{aligned} \quad (4)$$

Here, $K := \frac{k_1}{k_2 \Omega}$, and we again denote the new non-dimensional time by t (with an abuse of notation).

Remark 1. An alternative non-dimensionalization is obtained by dividing out $\frac{k_1}{\Omega}$ from Eq. (3) and by rescaling time accordingly; since the resulting equation is similar to (4), it is omitted here.

Eq. (4) can conveniently be written in matrix form as

$$\frac{d}{dt} \mathbf{P}(t) = \mathbf{M} \mathbf{P}(t), \quad (5)$$

where

$$\mathbf{P}(t) := \begin{pmatrix} \mathbb{P}(0, t) \\ \mathbb{P}(2, t) \\ \vdots \\ \mathbb{P}(2\Omega\alpha - 2, t) \\ \mathbb{P}(2\Omega\alpha, t) \end{pmatrix}$$

and

$$\mathbf{M} := \begin{pmatrix} -g(0) & f(1)K & 0 & \cdots & \cdots & \cdots & 0 \\ g(0) & -f(1)K - g(1) & f(2)K & 0 & \cdots & \cdots & 0 \\ 0 & g(1) & -f(2)K - g(2) & f(3)K & \ddots & \cdots & 0 \\ \vdots & \ddots & \ddots & \ddots & \ddots & \ddots & \vdots \\ 0 & \cdots & \ddots & g(n-2) & -f(n-1)K - g(n-1) & f(n)K & 0 \\ \vdots & \cdots & \cdots & \ddots & \ddots & \ddots & \vdots \\ 0 & \cdots & \cdots & \cdots & 0 & g(\Omega\alpha - 1) & -f(\Omega\alpha)K \end{pmatrix}, \quad (6)$$

with

$$f(n) := 2n(2n-1) \quad \text{and} \quad g(n) := \Omega\alpha - n. \quad (7)$$

By Eq. (5), the $(n+1)$ -th row in the matrix \mathbf{M} corresponds to the equation for the probability $\mathbb{P}(2n, t)$ of the system being in a state with $2n$ molecules of A at time t . For that reason, in what follows, we will conveniently relabel each state with $n_A = 2n$ as n .

The exact solution of the CME, Eq. (5), can then be expressed as

$$\mathbf{P}(t) = \mathbf{E}^{-1} e^{\Lambda t} \mathbf{E} \mathbf{P}(0), \quad (8)$$

where Λ is a diagonal matrix whose entries are the eigenvalues of the transition state matrix \mathbf{M} , \mathbf{E} is the matrix of eigenvectors of \mathbf{M} , and \mathbf{E}^{-1} is its inverse.

While the above solution is formally exact, it is impossible in practice to find analytical (closed-form) expressions for \mathbf{E} and Λ for general values of $\Omega\alpha$ and K . Numerical integration of (5) – or, equivalently, the evaluation of (8) – for $\Omega\alpha$ and K fixed, on the other hand, does not provide insight into the asymptotics with respect to these parameters. Hence, there is a clear need for approximation techniques that allow one to infer the (dynamical and steady-state) properties of the probability distribution $\mathbf{P}(t)$ defined by (8). The approach developed in this article is perturbative in nature, in that we expand the exact solution of (5) in an asymptotic series in powers of K , for K sufficiently small. We shall perform this expansion in three steps: we first construct an approximation for the eigenvalue matrix Λ (Section 2.4); then, in Sections 4.1 and 4.2, we approximate the eigenvector matrix \mathbf{E} and its inverse \mathbf{E}^{-1} , respectively; finally, in Section 5, we combine the resulting formulae to obtain the desired approximation for $\mathbf{P}(t)$. We emphasize that our approximation for \mathbf{E} is based on the results developed in Section 3 which, in turn, rely heavily on concepts from graph theory [6]; see, in particular, Proposition 1. The eigenvalue matrix Λ , on the other hand, can be approximated algebraically in the context of the dimerization reaction considered here. However, in more complex reaction networks, that approximation may need to be graph-based, as well; cf. also Remark 3 below.

Remark 2. As $\mathbf{P}(t)$ is the solution of the linear differential Eq. (5) that is, moreover, a regular perturbation problem (in K), we expect \mathbf{P} to be a C^∞ smooth function of K . This expectation will be confirmed by our analysis, as we will show that all three matrices \mathbf{E} , Λ , and \mathbf{E}^{-1} involved in (8) are C^∞ smooth in K ; see Remarks 4 and 9 below. In particular, it will follow that \mathbf{P} admits an asymptotic series expansion in K , as claimed.

2.3 Significance and applicability

Before proceeding with our perturbative approach, we briefly discuss the physical significance and the practical applicability of the small- K limit in Eq. (4).

The physical significance is easily discerned. The inverse of k_2 defines the time-scale governing the dissociation of a dimer molecule B , whereas the inverse of $\frac{k_1}{\Omega}$ determines the time-scale on which the binding of two monomer molecules A occurs. Thus, K small simply implies a time-scale separation between these two processes.

The practical applicability of a small- K expansion can be seen as follows. For a given ratio of forward and reverse rate constants $\frac{k_1}{k_2}$, small values of K ensue if the reaction volume Ω is significantly larger than that ratio. To estimate how large Ω needs to be for our methodology to be of physical significance, we note that the range of the forward

(bimolecular) rate constant is approximately $10^6 - 10^9 M^{-1}s^{-1}$, where the upper and lower limits are relevant for diffusion-limited reactions and for reaction-limited ones, respectively [11]. Since well-mixed conditions are only compatible with reaction-limited dynamics [24], we choose $k_1 = 10^6 M^{-1}s^{-1}$. As for the reverse (unimolecular) rate constant, the typical range is given by $1 - 10^4 s^{-1}$ [11]. Hence, for $k_2 = 1 s^{-1}$, K is “small” if the reaction volume Ω is significantly larger than a cube of side length $0.1\mu m$; similarly, if we take $k_2 = 10^4 s^{-1}$, K is small if the volume is considerably larger than a cube of side length $6nm$. As intracellular compartments range in size from diameters of about $50nm$ to a few microns [2], it is clear that small values of K are compatible with the modeling of intracellular conditions. We also note that smallness of K places no restriction on the total number of monomers n_{tot} ; correspondingly, our expansion will be capable of capturing equally well scenarios with small or large molecule numbers, which is desirable.

Finally, we emphasize that our expansion is different from the conventional system-size expansion of the CME [35]. The latter is a large-volume expansion at constant macroscopic concentration, which, for the dimerization reaction, would imply taking the large- Ω limit at constant total monomer concentration α . (In other words, the total number of monomers n_{tot} would increase proportionately with the volume.) This scenario is typically referred to as the thermodynamic (or macroscopic) limit [16], and is the limit employed by the system-size expansion and by LNA, on which it is based; see again [35]. By contrast, our small- K expansion corresponds to the limit of large volumes at some fixed total number of monomers n_{tot} ; that limit is frequently more relevant in practice, since it potentially allows for small copy numbers of molecules, as it is often the case in living cells. The conceptual difference between the two expansions is illustrated in Fig. 1.

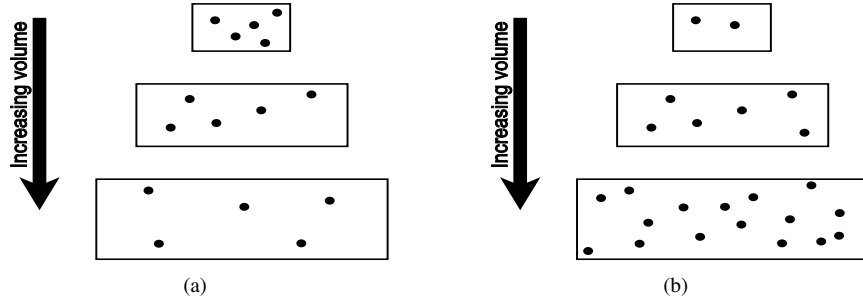


Figure 1: Illustration of the effects of a change in reaction volume. In panel (a), the total number of monomers is fixed for all volumes, which implies that the total monomer concentration decreases as the volume increases; in panel (b), the total number of monomers is increased proportionately with the reaction volume such that the total concentration remains constant. Case (a) is the one studied in this article, whereas case (b) corresponds to the well-studied thermodynamic (macroscopic) limit [35].

2.4 Eigenvalue expansion

In this subsection, we approximate the set of eigenvalues of the transition matrix \mathbf{M} defined in Eq. (6) by a series expansion in terms of the non-dimensional parameter K . As is well known, eigenvalues of \mathbf{M} are obtained by solving the eigenvalue equation

$$\det(\mathbf{M} - \lambda \mathbf{I}) = 0 \quad (9)$$

for λ . Expanding $\lambda = a_0 + a_1K + o(K)$ and omitting the $o(K)$ terms, we find

$$\mathbf{M}_\lambda := \mathbf{M} - \lambda \mathbf{I} = \begin{pmatrix} -g(0) - a_0 - a_1K & f(1)K & 0 & \cdots & 0 \\ g(0) & -f(1)K - g(1) - a_0 - a_1K & f(2)K & \ddots & \vdots \\ 0 & \ddots & \ddots & \ddots & 0 \\ \vdots & \ddots & \ddots & \ddots & \vdots \\ 0 & \cdots & 0 & g(\Omega\alpha - 1) & -f(\Omega\alpha)K - a_0 - a_1K \end{pmatrix}.$$

We can now apply the determinant property

$$\det(\mathbf{M}_\lambda) = \sum_{\sigma \in \mathcal{S}} \text{sgn}(\sigma) \prod_{n=0}^{\Omega\alpha} \mathbf{M}_\lambda[n, \sigma(n)], \quad (10)$$

where \mathcal{S} is the set of all permutations of $\{0, 1, \dots, \Omega\alpha\}$ and $\mathbf{M}_\lambda[i, j]$ denotes the (i, j) -th entry in \mathbf{M}_λ .

The advantage of employing the expression in (10) when evaluating the determinant of \mathbf{M}_λ lies in the fact that most of the terms in the above sum are either zero or $o(K)$ and, hence, negligible to the order considered here. In fact, the only non-zero permutations in (10) will be the ones that exchange pairs of neighboring numbers $(n, n+1)$. Each time a pair of such numbers is exchanged, the factor $\mathbf{M}_\lambda[n, n+1] \cdot \mathbf{M}_\lambda[n+1, n] = Kf(n+1)g(n)$ appears in the product in Eq. (10). Consequently, the only permutation that contributes to the constant term in (10) is the identity. Similarly, the only permutations contributing to the $O(K)$ term are the ones that exchange pairs of neighboring numbers, *i.e.*, all cyclic permutations of the form $\sigma_n := (n \ n+1)$, with $n = 0, 1, \dots, \Omega\alpha - 1$. Thus, it follows that Eq. (10) can be written as

$$\begin{aligned} \det(\mathbf{M}_\lambda) &= \prod_{i=0}^{\Omega\alpha} \mathbf{M}_\lambda[i, i] + \sum_{j=0}^{\Omega\alpha-1} \text{sgn}(\sigma_j) \prod_{i=0}^{\Omega\alpha} \mathbf{M}_\lambda[i, \sigma_j(i)] + o(K) \\ &= \prod_{i=0}^{\Omega\alpha} [-g(i) - a_0 - f(i)K - a_1K] - K \sum_{j=0}^{\Omega\alpha-1} f(j+1)g(j) \prod_{\substack{i=0 \\ i \neq j, i \neq j+1}}^{\Omega\alpha} [-g(i) - a_0] + o(K), \end{aligned} \quad (11)$$

where the functions f and g are defined in Eq. (7). (Here and in the following, conventional “big- O ” notation indicates exact knowledge of the order in K of a given expression, whereas “small o ” is used otherwise, as in the case of the error resulting from the truncation at $O(K)$ above.)

For Eq. (9) to be satisfied, the terms in the expansion in (11) must equal zero separately, *i.e.*, order-by-order in K . Setting the $O(1)$ term to zero, we find the $\Omega\alpha + 1$ solutions

$$a_0^n := -g(n) = n - \Omega\alpha, \quad \text{with } n = 0, 1, \dots, \Omega\alpha.$$

Next, we observe that

$$\prod_{i=0}^{\Omega\alpha} [-g(i) - a_0^n - f(i)K - a_1^n K] = [-f(n)K - a_1^n K] \prod_{\substack{i=0 \\ i \neq n}}^{\Omega\alpha} [-g(i) - a_0^n] + o(K)$$

and

$$K \sum_{j=0}^{\Omega\alpha} f(j+1)g(j) \prod_{\substack{i=0 \\ i \neq j, i \neq j+1}}^{\Omega\alpha} [-g(i) - a_0^n] = K \sum_{\substack{j=n-1 \\ j=n}}^{\Omega\alpha} f(j+1)g(j) \prod_{\substack{i=0 \\ i \neq j, i \neq j+1}}^{\Omega\alpha} [-g(i) - a_0^n] + o(K).$$

Hence, for the $O(K)$ terms in Eq. (11) to evaluate to zero, we require

$$a_1^n = - \left[f(n) + \frac{f(n)g(n-1)}{g(n) - g(n-1)} + \frac{f(n+1)g(n)}{g(n) - g(n+1)} \right]; \quad (12)$$

the corresponding eigenvalue of \mathbf{M} will be denoted by $\lambda_n = a_0^n + a_1^n K + o(K)$. (Here, we remark that $f(0)g(-1) = 0 = f(\Omega\alpha + 1)g(\Omega\alpha)$, which is due to $f(0) = 0 = g(\Omega\alpha)$; cf. again Eq. (7).)

Remark 3. We note that a_1^n consists of three terms which correspond to the identity, the “left” permutation $(n-1\ n)$, and the “right” permutation $(n\ n+1)$, respectively; all other permutations annihilate the last product in the second line of Eq. (11), as $a_0^n = -g(n)$. Interpreting the above observation in a graph-theoretic context [6], we may conclude that the expansion for λ_n only depends on neighboring vertices in the graph associated to \mathbf{M} , at least to the order considered here; cf. also Section 4, where we will determine a graph-based approximation for the corresponding eigenvectors, as well as Section 6, where the extension of the approach developed in this article to more general reaction networks is discussed.

Substituting the definition of the functions f and g from Section 2.2 into Eq. (12), we obtain

$$a_1^n := -2(\Omega\alpha - n)(4n + 1), \quad \text{with } n = 0, 1, \dots, \Omega\alpha,$$

for the first-order term in the expansion of λ_n .

In sum, a compact expression for the n -th eigenvalue of the transition matrix \mathbf{M} is thus given by

$$\lambda_n = (n - \Omega\alpha) + 2(n - \Omega\alpha)(4n + 1)K + o(K), \quad \text{for } n = 0, 1, \dots, \Omega\alpha. \quad (13)$$

Remark 4. It follows from standard linear algebra [3] that λ_n is C^∞ smooth in K ; hence, the expansion in (13) can in principle be taken to any order. However, we note that this expansion may only be an asymptotic series in K ; in other words, it may not be convergent.

3 Main result

In this section, we develop the main theoretical result of this article, a graph-based algorithm for calculating the adjoint matrix of a given square matrix that is inspired by “method (B)” of [30]. Our proof of Proposition 1 below relies on an application of the Laplace expansion for the determinant of a matrix which also underlies the analysis in [30] and which is, to the best of our knowledge, novel in the context of the CME, as considered here. We begin by recalling that any non-zero column of the adjoint of $\mathbf{M} - \lambda\mathbf{I}$ is an eigenvector of the matrix \mathbf{M} , corresponding to the eigenvalue λ . In the subsequent section, we will apply our approach to the dimerization reaction introduced in Section 2 to obtain a series expansion (in K) for the matrix of eigenvectors of the transition state matrix defined in Eq. (6).

3.1 Preliminaries

The next (well-known) result on the relationship between a given square matrix and its adjoint matrix follows directly from Laplace’s expansion of the determinant of a matrix; see, *e.g.*, [3] for a proof.

Lemma 1. *For any (square) matrix \mathbf{H} ,*

$$\mathbf{H} \cdot \text{Adj}(\mathbf{H}) = \det(\mathbf{H})\mathbf{I},$$

where $\text{Adj}(\mathbf{H})$ is the adjoint matrix of \mathbf{H} .

In particular, if λ is an eigenvalue of some matrix \mathbf{M} , then $\det(\mathbf{M} - \lambda\mathbf{I}) = 0$. Hence, by Lemma 1, $(\mathbf{M} - \lambda\mathbf{I}) \cdot \text{Adj}(\mathbf{M} - \lambda\mathbf{I}) = \mathbf{0}$ or $\mathbf{M} \cdot \text{Adj}(\mathbf{M} - \lambda\mathbf{I}) = \lambda \text{Adj}(\mathbf{M} - \lambda\mathbf{I})$, *i.e.*, every non-zero column of $\text{Adj}(\mathbf{M} - \lambda\mathbf{I})$ is an eigenvector of \mathbf{M} . (Here, we note that a non-zero column always exists when λ has geometric multiplicity one; cf. [4].)

3.2 Calculation of adjoint

We now extend “method (B),” as developed in [30], with the aim of obtaining an algorithmic procedure for the calculation of the adjoint of a given matrix. In [30], the Laplace expansion is applied to adjacency matrices of “chemical” graphs, *i.e.*, to graphs in which vertices correspond to the atoms in the compound under consideration, while edges represent chemical bonds between those atoms. However, their results only hold for non-directed graphs; moreover, they obtain no explicit formula for the sign associated with a given path. By contrast, our extension is valid for directed graphs, and we do find a simple expression for the corresponding sign, as specified below.

Remark 5. In the following, we will assume familiarity with basic concepts and notions from graph theory, which we will not define explicitly here; the reader is referred to [6] for details.

Proposition 1. *Let G be the graph with adjacency matrix \mathbf{M} , and let \mathbf{A} be the adjoint matrix of $\mathbf{M} - \lambda \mathbf{I}$, with λ an eigenvalue of \mathbf{M} . Then,*

$$\mathbf{A}[i, j] = \begin{cases} Q(G \setminus \{i\}, \lambda) & \text{if } i = j, \\ \sum_{\mathcal{P}_{ij}} (-1)^{\ell(\mathcal{P}_{ij})} \omega(\mathcal{P}_{ij}) Q(G \setminus \mathcal{P}_{ij}, \lambda) & \text{otherwise,} \end{cases} \quad (14)$$

where the sum is calculated over all paths \mathcal{P}_{ij} between the vertices $i, j \in V(G)$. Here, $V(G)$ is the set of vertices in G , $\ell(\mathcal{P}_{ij})$ denotes the length of (or number of edges in) \mathcal{P}_{ij} , $\omega(\mathcal{P}_{ij})$ is the product of the weights of the edges in \mathcal{P}_{ij} , and $Q(G, \lambda)$ is the characteristic polynomial of the graph G , expressed in terms of λ , with the additional requirement that $Q(\emptyset, x) = 1$.

Proof. The proof consists in applying Laplace's expansion alternatively to the rows and the columns of $\mathbf{M} - \lambda \mathbf{I}$ until the problem is reduced to finding the characteristic polynomial $Q(G \setminus \mathcal{P}_{ij}, \lambda)$ of the graph $G \setminus \mathcal{P}_{ij}$, *i.e.*, the determinant of the adjacency matrix corresponding to $G \setminus \mathcal{P}_{ij}$ minus $\lambda \mathbf{I}$.

Since the assertion is trivial when $i = j$, we only consider the case where $i \neq j$. Let $\mathbf{H} := \mathbf{M} - \lambda \mathbf{I}$; then, we denote by $\mathcal{H}_{r_1, r_2, r_3, \dots}^{c_1, c_2, c_3, \dots}$ the matrix that is obtained from \mathbf{H} by elimination of rows r_1, r_2, r_3, \dots and of columns c_1, c_2, c_3, \dots . Moreover, we will refer to a particular row or column in the sub-matrix $\mathcal{H}_{r_1, r_2, r_3, \dots}^{c_1, c_2, c_3, \dots}$ not by its index in $\mathcal{H}_{r_1, r_2, r_3, \dots}^{c_1, c_2, c_3, \dots}$, but by its original index in the matrix \mathbf{H} . (Thus, for instance, when referring to column 2 in matrix \mathcal{H}_1^1 , we actually mean the first column of that matrix, as \mathcal{H}_1^1 is obtained from \mathbf{H} by elimination of the first row and the first column.)

Now, the (i, j) -th entry $\mathbf{A}[i, j]$ of the adjoint matrix \mathbf{A} of \mathbf{H} equals the cofactor $\mathbf{C}[j, i]$ of \mathbf{H} , which is defined as the determinant of the matrix \mathcal{H}_j^i times $(-1)^{i+j}$ [3]. We apply the Laplace expansion over row i of \mathcal{H}_j^i , *i.e.*, over the i -th row of \mathbf{H} . Since the only non-zero terms in that row are the neighbors of vertex i in G , we have

$$\det(\mathcal{H}_j^i) = \sum_{x_1 \sim i} (-1)^{s_{x_1}} \mathbf{H}[i, x_1] \det(\mathcal{H}_{j,i}^{i, x_1}),$$

where s_{x_1} is the sum of the actual position of row i and column x_1 in matrix \mathcal{H}_j^i , with $x_1 \sim i$ denoting the neighboring vertices of i in G . Moreover, we recall that $\mathbf{H}[i, x_1]$ is the weight of the edge (i, x_1) connecting i and x_1 .

Let us now fix $x_1 \sim i$. We again apply Laplace's expansion over row x_1 of $\mathcal{H}_{j,i}^{i, x_1}$, obtaining

$$\det(\mathcal{H}_{j,i}^{i, x_1}) = \sum_{\substack{x_2 \sim x_1 \\ x_2 \neq i}} (-1)^{s_{x_2}} \mathbf{H}[x_1, x_2] \det(\mathcal{H}_{j,i,x_1}^{i, x_1, x_2});$$

here, s_{x_2} is the sum of the actual position of row x_1 and column x_2 in matrix $\mathcal{H}_{j,i}^{i, x_1}$.

Iterating this procedure p times gives

$$\det(\mathcal{H}_{j,i,x_1,x_2,\dots,x_{p-2}}^{i,x_1,x_2,\dots,x_{p-1}}) = \sum_{\substack{x_p \sim x_{p-1} \\ x_p \neq i, x_1, \dots, x_{p-2}}} (-1)^{s_{x_p}} \mathbf{H}[x_{p-1}, x_p] \det(\mathcal{H}_{j,i,x_1,x_2,\dots,x_{p-2},x_{p-1}}^{i,x_1,x_2,\dots,x_{p-1},x_p}),$$

where s_{x_p} is the sum of the actual position of row x_{p-1} and column x_p in matrix $\mathcal{H}_{j,i,x_1,x_2,\dots,x_{p-1}}^{i,x_1,x_2,\dots,x_{p-1}}$.

Clearly, performing the above iteration corresponds to following all paths in G that originate from vertex i . We continue until one of the following two cases occurs:

1. $x_p = j$;
2. the only neighbors of x_p are in $\{i, x_1, \dots, x_{p-1}\}$.

In the first case, we have managed to eliminate the same rows and columns $i, j, x_1, \dots, x_{p-1}$, *i.e.*, we have reduced the problem to finding the determinant of the matrix $\mathcal{H}_{i, j, x_1, \dots, x_{p-1}}^{i, j, x_1, \dots, x_{p-1}}$ that corresponds to the characteristic polynomial $Q(G \setminus \mathcal{P}, \lambda)$, with \mathcal{P} being the path $\{i, x_1, \dots, x_{p-1}, j\}$; in other words, we have found one path in the sum in (14). In the second case, row x_p only contains zero terms; thus, the resulting determinant is zero. (An illustration of the above procedure can be found in Example 1 below.)

Finally, the sign in front of a path $\mathcal{P} = \{x_0, x_1, \dots, x_d\}$ with $x_0 := i$ and $x_d := j$ is given by the product $(-1)^{i+j} \prod_{p=1}^d (-1)^{s_{x_p}}$. Hence, we need to find $i + j + \sum_{p=1}^d s_{x_p} \pmod 2$. Let us define

$$m_{\beta, \gamma}^{\mathcal{P}} := \begin{cases} 1 & \text{when } x_\gamma < x_\beta, \\ 0 & \text{when } x_\beta < x_\gamma \end{cases}$$

for $\beta, \gamma \in \{0, 1, \dots, d\}$, and let

$$\mathbf{H}_p^{\mathcal{P}} := \begin{cases} \mathcal{H}_j^i & \text{for } p = 1, \\ \mathcal{H}_{j, i, x_1, x_2, \dots, x_{p-2}}^{i, x_1, x_2, \dots, x_{p-1}} & \text{for } p > 1. \end{cases}$$

We have already shown that $s_{x_p} = r_p^{\mathcal{P}}(x_{p-1}) + c_p^{\mathcal{P}}(x_p)$, where $r_p^{\mathcal{P}}(x)$ and $c_p^{\mathcal{P}}(x)$ denote the actual row and column index of x , respectively, in $\mathbf{H}_p^{\mathcal{P}}$. It is easy to see that

$$r_p^{\mathcal{P}}(x_{p-1}) = x_{p-1} - m_{p-1, d}^{\mathcal{P}} - \sum_{r=0}^{p-2} m_{p-1, r}^{\mathcal{P}} \quad \text{and} \quad c_p^{\mathcal{P}}(x_p) = x_p - \sum_{r=0}^{p-1} m_{p, r}^{\mathcal{P}}.$$

Summing over all p , we obtain

$$\sum_{p=1}^d s_{x_p} = i + j + \sum_{p=1}^{d-1} x_p + \sum_{p=2}^d x_{p-1} - \sum_{p=0}^{d-1} m_{p, d}^{\mathcal{P}} - \sum_{p=1}^{d-1} \sum_{r=0}^{p-1} m_{p, r}^{\mathcal{P}} - \sum_{p=1}^d \sum_{r=0}^{p-1} m_{p, r}^{\mathcal{P}}.$$

Taking the result modulo 2, one finds

$$\sum_{p=1}^d s_{x_p} \pmod 2 \equiv i + j - \sum_{p=0}^{d-1} m_{p, d}^{\mathcal{P}} - \sum_{r=0}^{d-1} m_{d, r}^{\mathcal{P}} \pmod 2 \equiv i + j + d.$$

Hence, we have

$$i + j + \sum_{p=1}^d s_{x_p} \pmod 2 \equiv d,$$

which concludes the proof. □

Remark 6. Proposition 1 implies, in particular, that the eigenvectors of a matrix \mathbf{M} which depends smoothly on a parameter K and whose eigenvalues are all distinct are C^∞ smooth in K : by Section 3.1, any non-zero column of $\text{Adj}(\mathbf{M} - \lambda \mathbf{I})$ yields an eigenvector corresponding to a given eigenvalue λ ; the proposition affirms that every entry of this adjoint is proportional to a characteristic polynomial which is C^∞ smooth in K .

We now illustrate the proof of Proposition 1 by studying a simple example.

Example 1. Consider the matrix

$$\mathbf{M} = \begin{pmatrix} * & 1 & 1 & 0 & 0 \\ 1 & * & 0 & 1 & 0 \\ 1 & 0 & * & 1 & 1 \\ 0 & 1 & 1 & * & 1 \\ 0 & 0 & 1 & 1 & * \end{pmatrix}$$

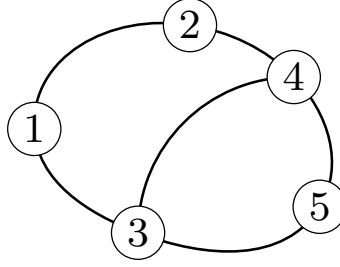


Figure 2: Graph G associated to the matrix \mathbf{M} defined in Fig. 3. The paths connecting 4 and 1 are given by $\{4, 2, 1\}$, $\{4, 3, 1\}$, and $\{4, 5, 3, 1\}$, corresponding to the sub-matrices in (a), (b), and (d), respectively, in Fig. 3. The sub-matrix in (c) corresponds to the path $\{4, 3, 5\}$ and equals zero, since that path does not end in 1.

and its associated undirected graph G , as shown in Fig. 2. (Here, we ignore the values on the diagonal of \mathbf{M} , as those would correspond to “loops” in the graph.) We intend to calculate the term $\mathbf{A}[4, 1]$, where $\mathbf{A} := \text{Adj}(\mathbf{M})$; in particular, retracing the procedure developed in the proof of Proposition 1, we will show that $\mathbf{A}[4, 1]$ depends on the determinants of the sub-matrices associated to the graphs $G \setminus \mathcal{P}$ for all paths \mathcal{P} connecting vertices 1 and 4.

Hence, we need to find the cofactor C_{14} of \mathbf{M} which, by definition, equals the determinant of the topmost matrix in Fig. 3, ignoring again any greyed-out entries. Applying the Laplace expansion of the determinant over row 4 – the crossed-out row in that same matrix – we decompose the original determinant into the sum of determinants of the three sub-matrices (left, center, and right) shown in the second row in Fig. 3; the sign of each term in the sum depends on the position at which we are applying the cofactor. In the context of the graph G given in Fig. 2, each of these sub-matrices corresponds to a neighbor of vertex 4, as indicated by a non-zero term in row 4 of \mathbf{M} . (Following the convention in the above proof, we also include greyed-out rows when counting.) Specifically, the circled numbers represent, respectively, the second, third, and fifth entries in row 4, or, equivalently, vertices 2, 3, and 5 in G . (We remark that, when considering weighted graphs, each of the determinants involved must additionally be multiplied by the weight of the corresponding edge.)

Next, we apply another Laplace expansion to each of the three sub-matrices in the second row in Fig. 3 which, incidentally, do not themselves have any graph-theoretical meaning.

1. *Left matrix:* we expand the determinant over row 2 and find the one non-zero entry corresponding to vertex 1, the only remaining neighbor of 2. That is the vertex we intended to reach; in fact, the resulting sub-matrix (a) in Fig. 3 corresponds to the adjacency matrix of the graph $G \setminus (4, 2, 1)$. (We note that all diagonal entries have fallen into place, since we eliminated rows and columns with the same indices 1, 2, and 4.)
2. *Center matrix:* expanding over row 3, we find two non-zero values, corresponding to vertices 1 and 5, which are the remaining neighbors of 3. The cofactor over $(3, 1)$ results in sub-matrix (b) in Fig. 3, which is the adjacency matrix of $G \setminus (4, 3, 1)$; again, all diagonal entries are correctly placed. The cofactor over $(3, 5)$, on the other hand, yields sub-matrix (c), whose determinant is 0, since vertex 5 has no neighbors other than the already considered vertices 4 and 3; thus, its corresponding row only contains zero entries.
3. *Right matrix:* expanding over row 5, we find that only the third entry is non-zero, which gives the rightmost matrix in the third row of matrices in Fig. 3. Expanding one more time over row 3, we obtain sub-matrix (d), which corresponds to the graph $G \setminus (4, 5, 3, 1)$, i.e., to the vertex 2 itself.

In sum, it is instructive to verify how, in following the above procedure, we have covered all paths between vertices 4 and 1 in the graph G shown in Fig. 2.

While we intend to approximate the “full” eigenvector matrix \mathbf{E} that is associated with a given matrix \mathbf{M} , the required computational effort is reduced by the observation that it suffices to determine one column of $\text{Adj}(\mathbf{M} - \lambda \mathbf{I})$ for each eigenvalue λ of \mathbf{M} . Moreover, we note that no assumption is made in Proposition 1 on the order (in K) of the expressions involved in the evaluation of that adjoint; in fact, as we will show below, many of the paths \mathcal{P}_{ij} occurring

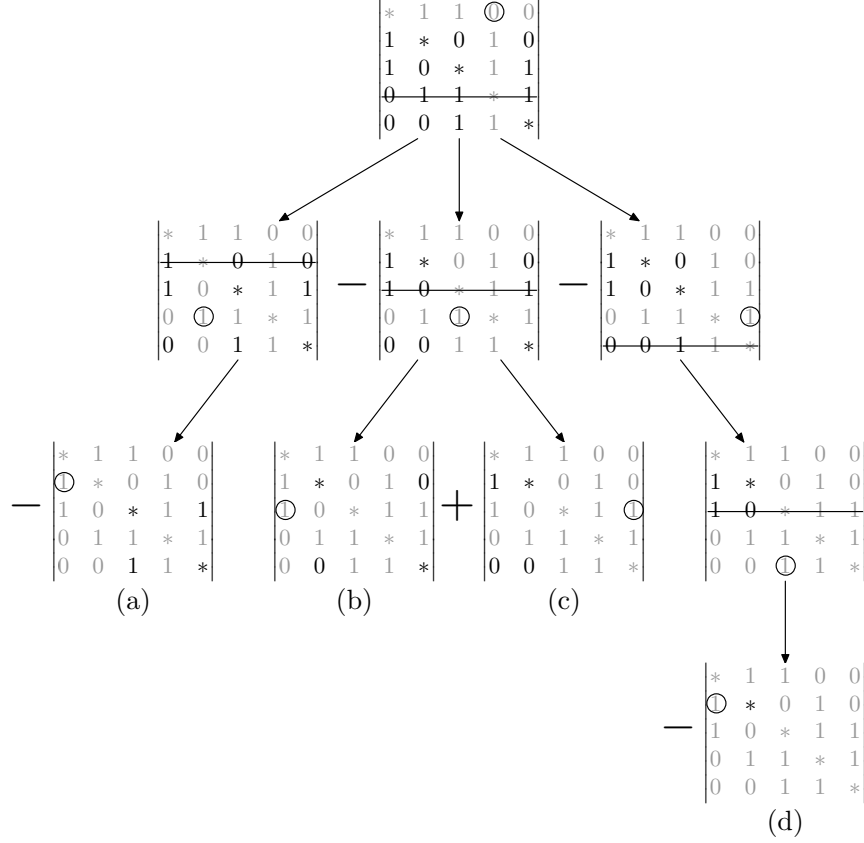


Figure 3: Illustration of the proof of Proposition 1. Our aim is to calculate $\mathbf{A}[4, 1]$: greyed-out entries have been removed from the matrix, crossed-out rows are the ones we are applying the Laplace expansion to, and circled entries indicate the calculation of a cofactor. The corresponding graph G is shown in Fig. 2.

in Eq. (14) are of higher order and can hence be neglected when applying the (very general) result of the proposition to the dimerization reaction considered in Section 2.

4 Dimerization revisited

In this section, we apply the results of the previous section to the reaction $A + A \xrightleftharpoons[k_2]{k_1} B$, *i.e.*, to the corresponding transition state matrix \mathbf{M} which is defined in (6). The graph of that reaction, which we shall denote by G_d , is illustrated in Fig. 4.

We remark that there is a natural correspondence between the eigenvalues of the matrix \mathbf{M} and the vertices of the associated graph G_d . In fact, for $K = 0$, \mathbf{M} reduces to a triangular matrix; hence, the n -th eigenvalue λ_n equals the element $\mathbf{M}[n, n]$ on the diagonal of \mathbf{M} which, in turn, corresponds to the n -th vertex in the graph G_d . Similarly, for $K > 0$, we assign to $n \in V(G_d)$ the eigenvalue whose leading-order term is given by $\mathbf{M}[n, n]$; we recall the corresponding series expansion (in K) for λ_n , Eq. (13), from Section 2.4.

4.1 Eigenvector matrix

We now discuss how the methodology developed in Section 3 can be applied to approximate (to first order in K) the matrix of eigenvectors \mathbf{E} of the transition matrix \mathbf{M} . As the eigenvalues λ_n of \mathbf{M} are distinct, with $n = 0, 1, \dots, \Omega\alpha$, we have $\Omega\alpha + 1$ corresponding eigenvectors; see again Section 2.4.

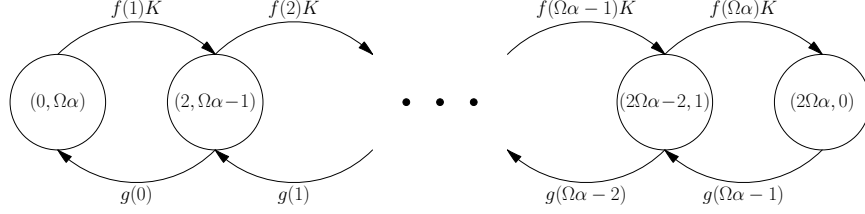


Figure 4: Graph associated to the transition state matrix \mathbf{M} defined in Eq. (6). The vertices correspond to all possible states in the system, while the edges are weighted with the transition probabilities; specifically, the weight of the edge connecting states i and j equals the probability of going from state j to i . (No edge is drawn when that probability is zero.) Although this notation may seem counterintuitive, it is consistent with much of the relevant literature; see, e.g., [35, 13].

Next, we note that, for each pair of vertices $i, j \in V(G_d)$, there exists only one path \mathcal{P}_{ij} connecting i and j ; cf. Fig. 4. Hence, the weight $\omega(\mathcal{P}_{ij})$ of that path is given by

$$\omega(\mathcal{P}_{ij}) = \prod_{r=i}^{j-1} \omega((r, r+1)) = \prod_{r=i}^{j-1} \mathbf{M}[r, r+1] = K^{j-i} \prod_{r=i}^{j-1} f(r+1) \quad \text{for } i < j \quad (15)$$

and by

$$\omega(\mathcal{P}_{ij}) = \prod_{r=j}^{i-1} \omega((r+1, r)) = \prod_{r=j}^{i-1} \mathbf{M}[r+1, r] = \prod_{r=j}^{i-1} g(r) \quad \text{for } i > j. \quad (16)$$

Remark 7. For $i = j$, we do not obtain a proper path in G_d , in the sense that we only have a vertex and no edges, which corresponds to the first case in Eq. (14).

Since we are interested in the asymptotics of $\omega(\mathcal{P}_{ij})$ up to and including first-order terms in K , it is evident from Eqs. (15) and (16) that we only need to consider the three cases where $i = j - 1$, $i = j$, and $i > j$ here. We require the following definition.

Definition 1. Given the eigenvalue λ_n of \mathbf{M} that corresponds to vertex $n \in V(G_d)$, we define

$$\lambda_n^+ := \lambda_n - \frac{f(n+1)g(n)}{g(n+1) - g(n)}K$$

and

$$\lambda_n^- := \lambda_n + \frac{f(n)g(n-1)}{g(n) - g(n-1)}K.$$

The definition of λ_n^\pm agrees with the expression for λ_n given in Eq. (12), up to one of the permutations considered there; specifically, we omit the “right” permutation in λ_n^+ and the “left” one in λ_n^- .

Proposition 2. Let $i, j \in \{1, \dots, \Omega\alpha - 1\}$, and let \mathcal{S}_{ij} be the set of vertices $\mathcal{S}_{ij} = \{\mu - 1, \mu, \mu + 1, \dots, \nu, \nu + 1\} \subseteq V(G_d)$, where $\mu = \min(i, j)$ and $\nu = \max(i, j)$. Then,

$$Q(G_d \setminus \mathcal{P}_{ij}, \lambda_n) = (\lambda_{\mu-1}^+ - \lambda_n)(\lambda_{\nu+1}^- - \lambda_n) \prod_{\substack{r=0 \\ r \notin \mathcal{S}_{ij}}}^{\Omega\alpha} (\lambda_r - \lambda_n) + o(K). \quad (17)$$

Proof. The statement follows by adapting the results of Section 2.4 to the graph $G_d \setminus \mathcal{P}_{ij}$ or, equivalently, to the characteristic polynomial of that graph. In particular, one finds that any eigenvalue associated with a vertex outside \mathcal{S}_{ij} agrees with the corresponding eigenvalue in G_d , up to and including terms of order K . Similarly, the eigenvalues λ_μ and λ_ν have the same $O(1)$ term in G_d and in $G_d \setminus \mathcal{P}_{ij}$; however, when determining the first-order term in K , one permutation drops out, as one of the neighboring vertices $\mu + 1$ and $\nu - 1$, respectively, does not enter the calculation anymore, leading to the introduction of $\lambda_{\mu-1}^+$ and $\lambda_{\nu+1}^-$, respectively, and to a discrepancy at $O(K)$. \square

When $\mu = 0$ or $\nu = \Omega\alpha$, Eq. (17) is still valid provided that the terms $(\lambda_{\mu-1}^+ - \lambda_n)$ and $(\lambda_{\nu+1}^- - \lambda_n)$, respectively, are ignored. Hence, defining $\mathbf{A}_n := \text{Adj}(\mathbf{M} - \lambda_n \mathbf{I})$ to be the adjoint matrix of $\mathbf{M} - \lambda_n \mathbf{I}$ and combining the results of Propositions 1 and 2, we can obtain the eigenvector of \mathbf{M} corresponding to λ_n from the n -th column of \mathbf{A}_n . Normalizing the resulting expression by dividing out a common (non-zero) factor of $\prod_{r=0}^{n-3} (\lambda_r - \lambda_n)$ from $\mathbf{A}_n[i, n]$, denoting the normalized column by $\tilde{\mathbf{A}}_n[i, n]$, and assuming that $n \neq 0, 1, \Omega\alpha$, for simplicity, we find

$$\tilde{\mathbf{A}}_n[i, n] = \begin{cases} -Kf(n)(\lambda_{n-2}^+ - \lambda_n)(\lambda_{n+1}^- - \lambda_n) \prod_{r=n+2}^{\Omega\alpha} (\lambda_r - \lambda_n) & \text{if } i = n-1; \\ (\lambda_{n-1}^+ - \lambda_n)(\lambda_{n+1}^- - \lambda_n)(\lambda_{n-2} - \lambda_n) \prod_{r=n+2}^{\Omega\alpha} (\lambda_r - \lambda_n) & \text{if } i = n; \\ (-1)^{i-n}(\lambda_{n-1}^+ - \lambda_n)(\lambda_{i+1}^- - \lambda_n)(\lambda_{n-2} - \lambda_n) \prod_{r=i+2}^{\Omega\alpha} (\lambda_r - \lambda_n) \prod_{r=n}^{i-1} g(r) & \text{if } n < i < \Omega\alpha; \\ (-1)^{\Omega\alpha-n}(\lambda_{n-1}^+ - \lambda_n)(\lambda_{n-2} - \lambda_n) \prod_{r=n}^{\Omega\alpha-1} g(r) & \text{if } i = \Omega\alpha; \\ o(K) & \text{otherwise.} \end{cases} \quad (18)$$

While Eq. (18) gives $\tilde{\mathbf{A}}_n[i, n]$ in its most compact form, the above expressions still contain terms that are insignificant to the order considered here, *i.e.*, terms of order K^2 and higher. In Appendix A, we quote alternative formulae that are truncated to $O(K)$ and that are hence more convenient for our purposes; moreover, we treat the cases when $n = 0, 1, \Omega\alpha$.

4.2 Inverse eigenvector matrix

In this subsection, we discuss how the inverse \mathbf{E}^{-1} of the matrix of eigenvectors \mathbf{E} , as defined in Eq. (8), can be approximated; to that end, we slightly adapt the approximation developed in the previous subsection.

We begin by observing that the left eigenvector \mathbf{y}_n of the transition matrix \mathbf{M} , corresponding to the eigenvalue λ_n , solves the equation

$$(\mathbf{M}^T - \lambda_n \mathbf{I})\mathbf{y}_n = \mathbf{0}, \quad \text{with } n = 0, 1, \dots, \Omega\alpha.$$

By standard linear algebra [3], \mathbf{E}^{-1} can be determined from the set of the left eigenvectors of \mathbf{M} ; specifically, \mathbf{E}^{-1} is the matrix whose rows are suitably normalized versions of these eigenvectors.

Remark 8. For future reference, we note that the vector $\mathbb{1}$ (as well as any non-zero multiple thereof) is always a left eigenvector of \mathbf{M} .

Given the result of Proposition 1, we need to determine (one column of) the matrix $\mathbf{B}_n := \text{Adj}(\mathbf{M}^T - \lambda_n \mathbf{I})$, as noted in Section 4.1. The only difference between the graph corresponding to \mathbf{M}^T and the one associated with \mathbf{M} lies in the orientation of the edges, which are inverted now. Hence, Eq. (17) remains valid, while the weights of the paths are again given by Eqs. (15) and (16), albeit with reversed conditions on the index i ; correspondingly, we have

$$\omega(\mathcal{P}_{ij}) = \prod_{r=j}^{i-1} \omega((r+1, r)) = \prod_{r=j}^{i-1} \mathbf{M}^T[r+1, r] = K^{i-j} \prod_{r=j}^{i-1} f(r+1) \quad \text{for } i > j$$

and

$$\omega(\mathcal{P}_{ij}) = \prod_{r=i}^{j-1} \omega((r, r+1)) = \prod_{r=i}^{j-1} \mathbf{M}^T[r, r+1] = \prod_{r=i}^{j-1} g(r) \quad \text{for } i < j.$$

The only cases of interest are $i = j + 1$, $i = j$, and $i < j$. For $n \neq 0, \Omega\alpha - 1, \Omega\alpha$, we find

$$\tilde{\mathbf{B}}_n[n, i] = \begin{cases} -Kf(n+1)(\lambda_{n-1}^+ - \lambda_n)(\lambda_{n+2}^- - \lambda_n) \prod_{r=0}^{n-2} (\lambda_r - \lambda_n) & \text{if } i = n+1; \\ (\lambda_{n-1}^+ - \lambda_n)(\lambda_{n+1}^- - \lambda_n)(\lambda_{n+2}^- - \lambda_n) \prod_{r=0}^{n-2} (\lambda_r - \lambda_n) & \text{if } i = n; \\ (-1)^{n-i}(\lambda_{i-1}^+ - \lambda_n)(\lambda_{n+1}^- - \lambda_n)(\lambda_{n+2}^- - \lambda_n) \prod_{r=0}^{i-2} (\lambda_r - \lambda_n) \prod_{r=i}^{n-1} g(r) & \text{if } 0 < i < n; \\ (-1)^n(\lambda_{n+1}^- - \lambda_n)(\lambda_{n+2}^- - \lambda_n) \prod_{r=i}^{n-1} g(r) & \text{if } i = 0; \\ o(K) & \text{otherwise.} \end{cases} \quad (19)$$

Here, $\tilde{\mathbf{B}}_n[n, i]$ is obtained from $\mathbf{B}_n[n, i]$ by dividing the latter by the non-zero product $\prod_{r=n+3}^{\Omega\alpha} (\lambda_r - \lambda_n)$, in analogy to the definition of $\tilde{\mathbf{A}}_n[i, n]$. As was the case in Section 4.1, the above Eq. (19) represents the most compact expression for $\tilde{\mathbf{B}}_n[n, i]$ which may, however, still contain insignificant (higher-order) terms. We refer the reader to Appendix A for the solution to order K , as well as for a discussion of the cases where $n = 0, \Omega\alpha - 1, \Omega\alpha$.

Finally, the inverse matrix \mathbf{E}^{-1} of \mathbf{E} is found from Eq. (19) by normalization. The normalizing values can be determined by multiplication of the matrix that is defined by (18) with the matrix given by (19). The result is a diagonal matrix, up to terms of order K . Dividing each left eigenvector of \mathbf{M} by the corresponding value in that matrix, we obtain \mathbf{E}^{-1} . This normalization procedure can easily be performed numerically for any fixed value of the non-dimensional parameter $\Omega\alpha$.

5 Numerical validation

We are now ready to construct our approximation to the solution $\mathbf{P}(t)$ of the CME, Eq. (5), as defined in (8). (For illustrative purposes, we restrict ourselves to the example of the dimerization reaction introduced in Section 2; in Section 6 below, we will indicate how our results can be extended to more general reaction networks.) To that end, we combine the results of Sections 2.4, 4.1, and 4.2: expanding the eigenvalues of \mathbf{M} as in Eq. (13), we construct the diagonal eigenvalue matrix Λ ; applying the expansions from Eqs. (18) and (19), we approximate the corresponding matrix of eigenvectors \mathbf{E} and its inverse \mathbf{E}^{-1} , respectively. Substituting into Eq. (8) and retaining terms of at most order K , we obtain the desired approximate solution.

Remark 9. Remark 6 and the derivation of Eqs. (18) and (19) above imply that both \mathbf{E} and its inverse \mathbf{E}^{-1} are C^∞ smooth in K , in all of their entries.

In panels (a) and (b) of Fig. 5, we compare the mean M and the variance V , respectively, of the number of monomer molecules, as calculated from our approximate solution (open circles) and the numerical solution of the CME, Eq. (5) (solid lines), for a total of 40 monomers and $K = 10^{-7}$. (Henceforth, we will refer to the latter as the “exact” solution of (5) for fixed values of $\Omega\alpha$ and K .) The two solutions are in excellent agreement – and are, in fact, indistinguishable on the scale of panels (a) and (b) in Fig. 5 – which strongly supports the validity of our perturbative approach. In panels (c) and (d) of Fig. 5, we show the corresponding relative error in the mean and the variance, respectively. (Here, the relative error is equal to the modulus of the absolute error, divided by the exact solution.) We remark that, in both cases, the relative error grows from zero to some maximum that is achieved at steady state, independently of initial conditions.

In Fig. 6, we plot the maximum absolute error in the mean and the variance of the number of monomer molecules – which are denoted by ε_M and ε_V , respectively – as a function of K for $\Omega\alpha$ equal to 5, 10, and 20. In all cases, the maximum absolute error scales like $O(K^2)$, which is consistent with our first-order truncation of the series expansion in K for the solution $\mathbf{P}(t)$ of the CME, Eq. (5).

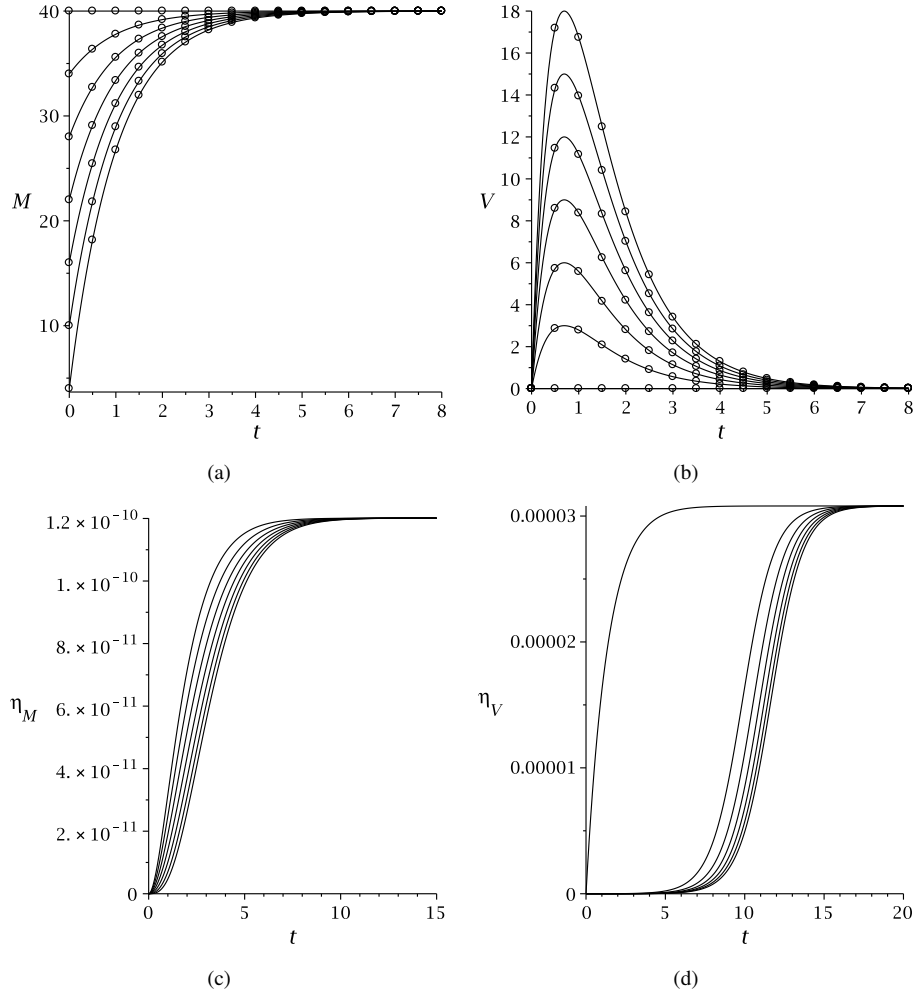


Figure 5: Comparison of the graph-based approximation and the exact (numerical) solution of Eq. (5). In panels (a) and (c), we plot the mean number M of monomer molecules and the relative error in the mean η_M as a function of time for different initial conditions; panels (b) and (d) show the variance V in the number of monomer molecules and the corresponding relative error η_V , respectively. The non-dimensional parameter $\Omega\alpha$ is fixed to 20, allowing for a maximum of 40 monomer molecules in the system, while $K = 10^{-7}$ throughout.

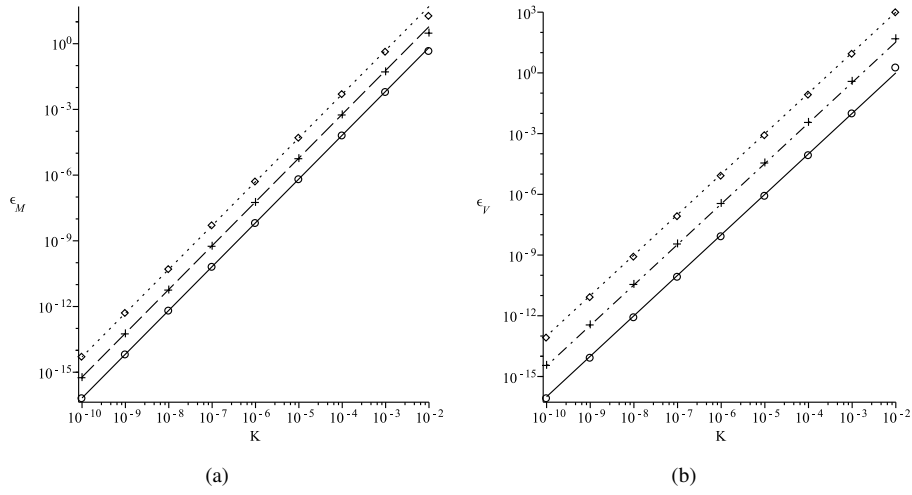


Figure 6: Maximum absolute error in the mean (ϵ_M) and the variance (ϵ_V) of the number of monomer molecules as a function of K , as shown in panels (a) and (b), respectively. Here, $\Omega\alpha$ is alternatively set to 5 (circles), 10 (crosses), and 20 (diamonds). The maximum error is attained when steady-state conditions ensue; in practice, we evaluated our approximate probability density at $t = 15$. The solid, dashed, and dotted lines represent $\frac{2}{3} \cdot 10^4 K^2$, $6 \cdot 10^4 K^2$, and $5 \cdot 10^5 K^2$ in panel (a) and $10^4 K^2$, $\frac{1}{3} \cdot 10^6 K^2$, and $10^7 K^2$ in panel (b), respectively. The initial condition is $\mathbb{P}(n_A = 0, t = 0) = 1$ in all cases.

5.1 Comparison with LNA

As discussed already in Section 2.3, LNA [35, 7] is based on an expansion procedure that is different from the perturbative approach developed in this article. Nevertheless, it is still possible to compare the two approaches for fixed values of the volume Ω , the total semi-concentration α , and the non-dimensional parameter K . A concise derivation of LNA for the dimerization reaction considered here can be found in Appendix B.

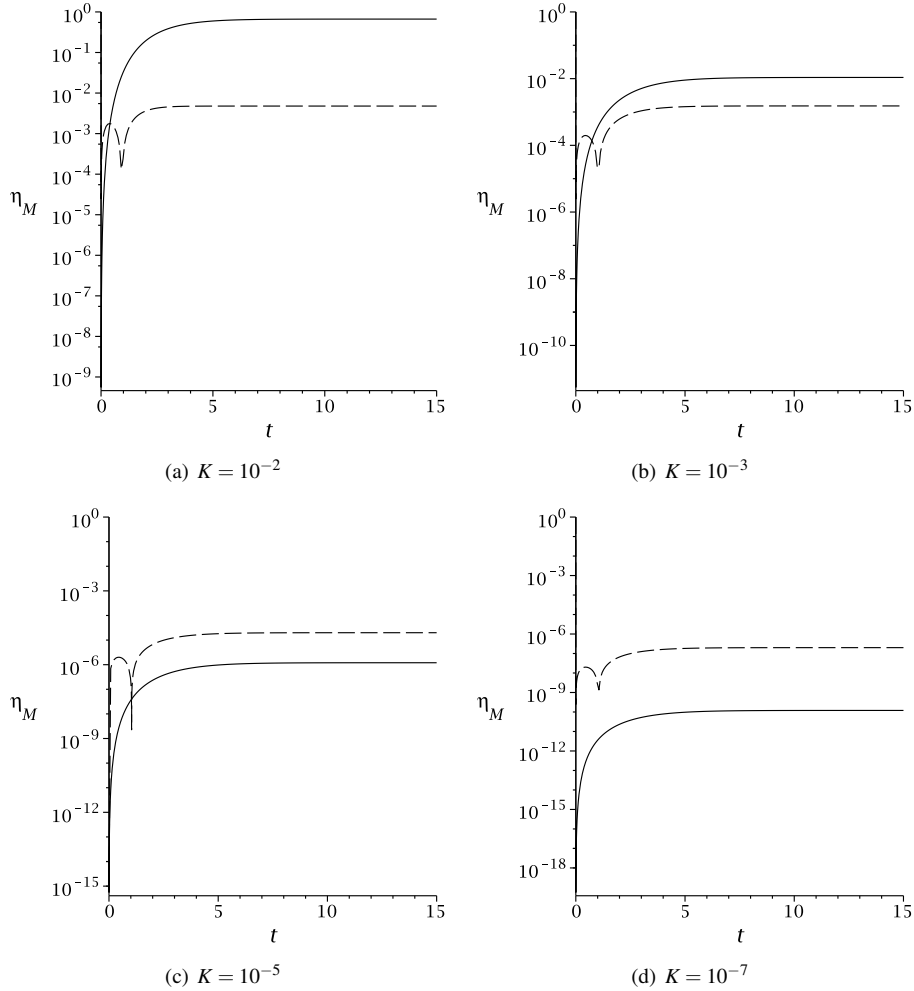


Figure 7: Relative error η_M in the mean of the number of monomer molecules as a function of time and for different values of K , as given by our perturbation approach (solid lines) versus LNA (dashed lines). The parameter $\Omega\alpha$ is fixed to 20 throughout. Although LNA performs better most of the time in panels (a) and (b), there is a short time interval during which our approach is superior. For sufficiently small K , the perturbative approach is more accurate than LNA for practically all times; see panels (c) and (d). (The sharp dips in the dashed graphs actually go down to zero, but are truncated here for aesthetic reasons. These dips correspond to times at which the difference between the exact and the approximate solution changes sign; see also [22].)

In Figs. 7 and 8, we compare the relative error in the mean and the variance that is predicted by the two approaches for several different values of K ; throughout, we set $\Omega\alpha = 20$, *i.e.*, we allow for a maximum of 40 monomer molecules in the system. We note that the mean concentrations according to LNA are the same as those obtained from the conventional rate equations. For very small $K = O(10^{-5})$, our perturbative approach outperforms LNA for practically all times, as seen in panels (c) and (d) of Figs. 7 and 8; however, for larger values of $K = O(10^{-3})$, it performs better

than LNA for short times only. Hence, it can be stated that our approach is always superior to LNA for K sufficiently small; moreover, this statement is independent of the number of molecules in the system.

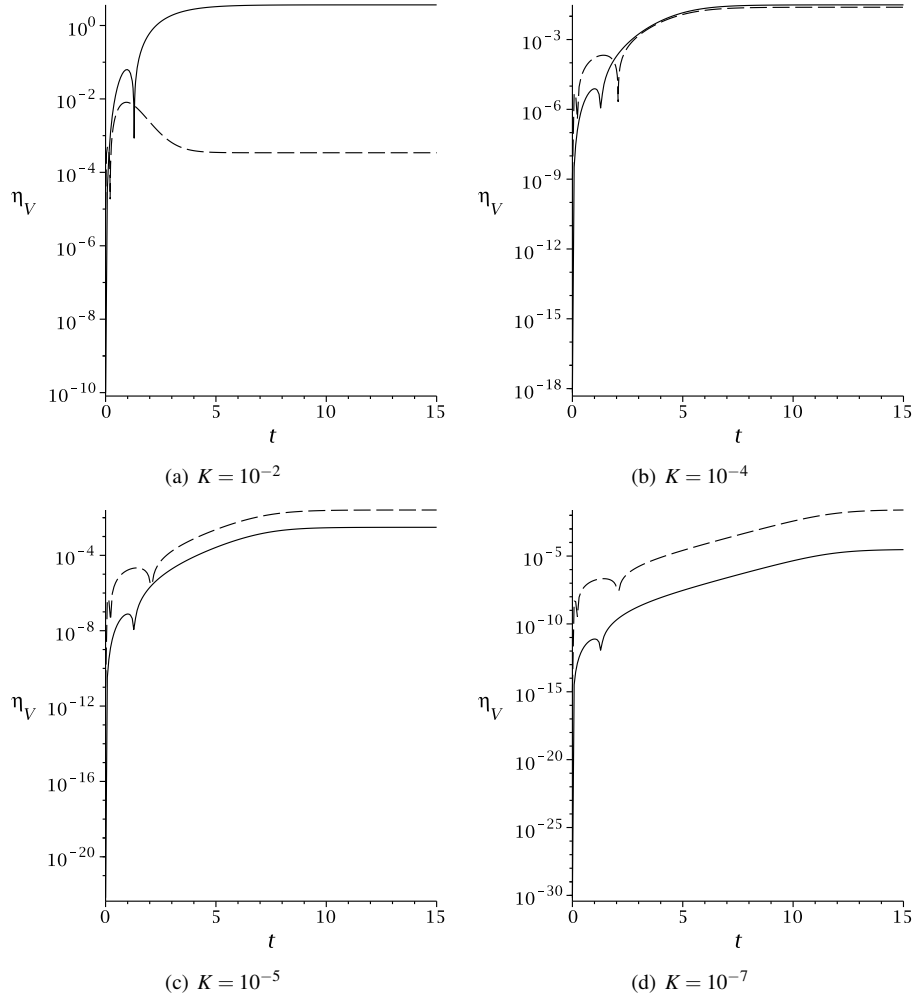


Figure 8: Relative error η_V in the variance of the number of monomer molecules as a function of time and for different values of K , as given by our perturbation approach (solid lines) versus LNA (dashed lines). The parameter $\Omega\alpha$ is fixed to 20 throughout. Although LNA performs better most of the time in panels (a) and (b), there is a short time interval during which our approach is superior. For sufficiently small K , the perturbative approach is more accurate than LNA for practically all times; see panels (c) and (d).

Next, we compare our perturbative expansion for the probability distribution $\mathbb{P}(n_A, t)$ of the number of monomer molecules with the approximation given by LNA, cf. Eq. (42), as well as with the distribution obtained from the standard stochastic simulation algorithm (SSA) [16]. (We note that, in all three cases, the height of the histogram for fixed n_A is calculated by integrating the corresponding density over the range $n_A - 1$ to $n_A + 1$; as indicated also in Appendix B, the continuous probability distribution resulting from LNA is discretized by this procedure and, hence, becomes directly comparable to the other two (discrete) distributions.) The result is shown in Fig. 9 for K fixed to 10^{-4} and three different values of t , the choice of which is motivated by the very fast convergence to steady state that is observed in the context of the probability distribution, as opposed to the moments considered earlier. We find that LNA is inaccurate both at short times and at long times, as seen in panels (a) and (c), while it performs reasonably well at intermediate times, as shown in panel (b); by contrast, our graph-based approximation achieves a uniformly

high accuracy throughout. The poor performance of LNA in this scenario is due to the fact that it predicts a Gaussian monomer distribution for all times, whereas the true distribution is highly skewed and non-Gaussian whenever the mean number of monomer molecules is close to the two natural boundaries, *i.e.*, to zero and to the total number of monomers in the system.

Our findings are validated by Fig. 10, where we show the Kullback-Leibler (K-L) divergence [5] of our approach (dashed line) and of LNA (solid line) with respect to the distribution obtained from SSA as a function of time. (For consistency with Fig. 9, we have again taken $K = 10^{-4}$, and we have assumed that no monomer molecules are present initially.) One observes that, for all times, the K-L divergence is significantly lower for our graph-based methodology than it is for LNA; correspondingly, for small values of K , the difference between the probability distribution predicted by our approach and the true solution of the CME, Eq. (2), is much smaller than the difference between the probability distribution predicted by LNA and the true solution.

Since, on the other hand, our methodology is perturbative, its accuracy deteriorates with increasing K , as illustrated in panel (a) of Fig. 11: when K is not sufficiently small, our series expansion for the distribution $\mathbb{P}(n_A, t)$ may become inconsistent; in other words, it may predict negative probabilities. Such inconsistencies are well-known in the literature, see, *e.g.*, [21] and the references therein for details: in general, the asymptotic expansion of a probability distribution is not a distribution itself and, hence, does not satisfy the non-negativity conditions required of the latter. Nevertheless, our approach can still yield a decent approximation for “intermediate” values of K when t is small, as seen in panel (b) of Fig. 11.

Remark 10. We note that the derivation of LNA in Appendix B is based on the original (dimensional) CME, Eq. (2), as is conventional, rather than on its non-dimensionalized equivalent in (4). In order to avoid a rescaling of time when comparing LNA with our approach, we have chosen $k_2 = 1$ throughout this section. (Clearly, the value of k_2 is irrelevant for the remainder of our analysis, as only the non-dimensional parameter K is considered.)

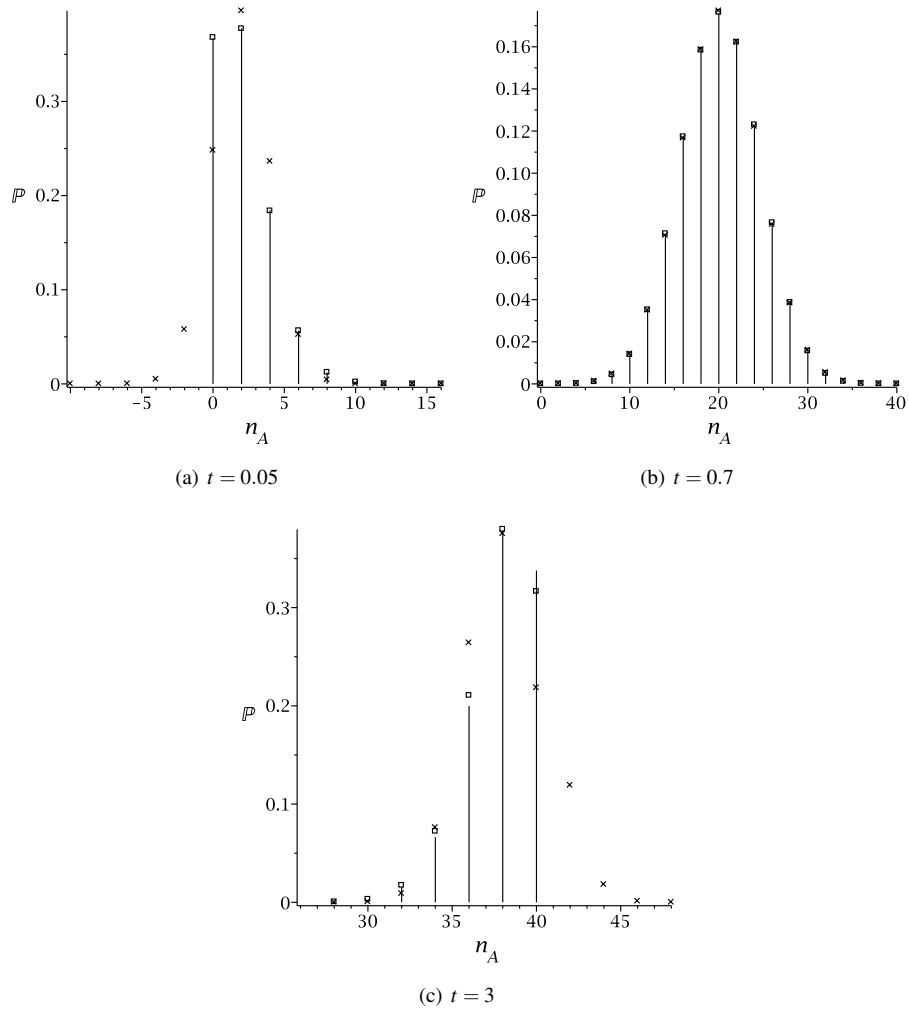


Figure 9: Comparison between the probability distribution obtained from SSA (histogram), our perturbative approach (squares), and LNA (crosses) for $\Omega\alpha = 20$ and $K = 10^{-4}$ fixed and three points in time. (The initial condition is set to $n_A = 0$ in all cases.) Our methodology agrees with SSA on the scale of the figure for small times, as seen in panel (a). As the distribution approaches steady state, the quality of the approximation decreases; yet, it still exceeds the accuracy achieved by LNA, as shown in panel (c).

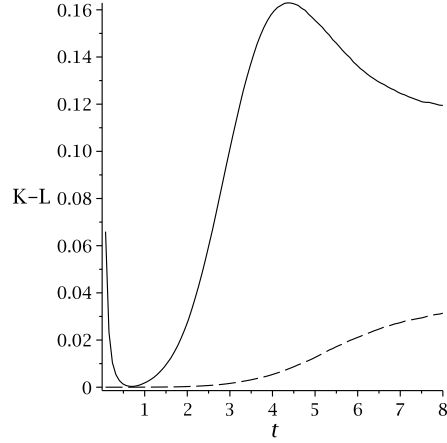


Figure 10: Kullback-Leibler (K-L) divergence of our approach (dashed line) and LNA (solid line) with respect to the distribution obtained from SSA, with $2 \cdot 10^5$ trajectories; here, we have fixed $\Omega\alpha = 20$ and $K = 10^{-4}$, and chosen $n_A = 0$ initially throughout. We observe that the K-L divergence of our approach is lower for all times.

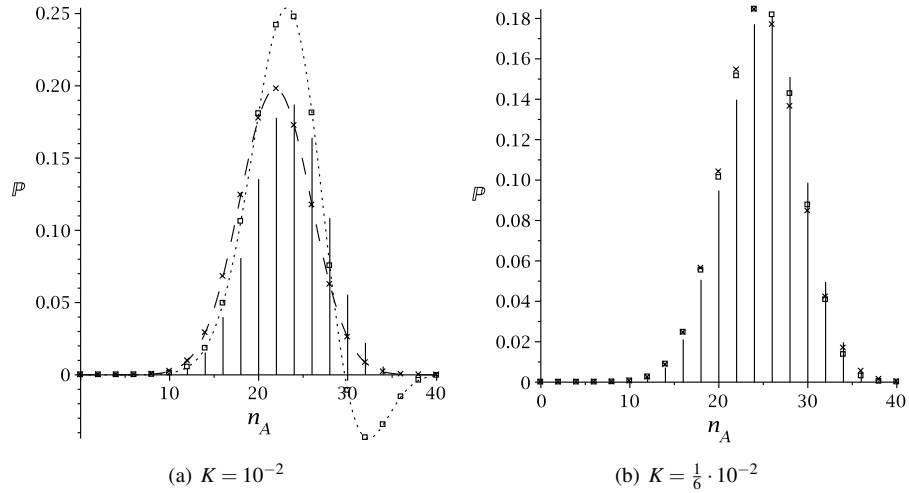


Figure 11: Comparison between the distribution obtained from SSA (histogram), our perturbative approach (squares), and LNA (crosses) for $\Omega\alpha = 20$ and $t = 1$ fixed and two different values of K . (As before, we assume that, initially, $n_A = 0$.) In panel (a), we have joined individual points with lines – dotted for our approach and dashed for LNA – to guide the reader’s eye.

6 General reaction networks

In this section, we briefly discuss how the graph-based approach developed in this article can be extended from the bimolecular (dimerization) reaction studied in Section 4 to more general sets of chemical reactions; an in-depth investigation will be the topic of an upcoming publication. We begin by noting that the CME for a continuous-in-time Markov chain will be of the general form

$$\frac{d}{dt}\mathbb{P}(\mathbf{n},t) = \sum_{\mathbf{n}'\sim\mathbf{n}} \{W(\mathbf{n}|\mathbf{n}')\mathbb{P}(\mathbf{n}',t) - W(\mathbf{n}'|\mathbf{n})\mathbb{P}(\mathbf{n},t)\}, \quad (20)$$

where $W(\mathbf{n}'|\mathbf{n})$ and $W(\mathbf{n}|\mathbf{n}')$ denote the transition probabilities of going from state \mathbf{n} to \mathbf{n}' and from state \mathbf{n}' to \mathbf{n} , respectively; see, *e.g.*, [35] for details.

We shall impose the following four conditions:

- (A) the stochastic process described by the CME, Eq. (20), can only contain a finite number of states;
- (B) the CME, Eq. (20), can be non-dimensionalized so that the resulting equation depends on a unique small (non-dimensional) parameter K ;
- (C) the corresponding transition matrix \mathbf{M} can be written as $\mathbf{M} = \mathbf{M}_0 + K\mathbf{M}_1$, where \mathbf{M}_0 is lower triangular (possibly after a relabeling of states);
- (D) the weight of cycles of length 2 in \mathbf{M} is $\Theta(K)$ (of exact order K), while cycles of length greater than 2 carry a weight of $o(K)$.

Remark 11. Condition (A) is imposed to ensure that Eq. (20) has a representation in matrix form, with a finite-dimensional transition matrix \mathbf{M} , and to avoid that the number of molecules of some species may become so large as to render the perturbation in K inconsistent; cf. condition (B). However, when condition (A) is not met, it is still possible to study open reaction networks – and the associated unbounded graphs G – either by applying our methodology to a truncation of G , or by modeling explicitly the corresponding external system and the interaction (via diffusion) between the two; see also [31].

Condition (B) is usually satisfied when considering reaction networks in very large or very small volumes, even if more than two reaction rates are involved: conveniently, the reaction volume is often simultaneously relevant to many reactions in a system. Hence, it sometimes suffices to fix all rate constants, and to take the limit of Ω going to zero or to infinity to obtain a unique small parameter and, thus, a separation of scales. Alternatively, letting several rate constants tend to infinity or to zero usually results in the presence of more than one small parameter in the system; thus, a fixed direction in parameter space must be imposed in that case for our approach to be applicable. Details can be found in Appendix C below; while we expect that most physically relevant reaction networks will satisfy condition (B) (at least in some parameter regime), a general characterization is beyond the scope of this article.

Condition (C) is equivalent to requiring that the graph associated to the “fast system” – which, incidentally, has the adjacency matrix \mathbf{M}_0 – is acyclic.

Finally, condition (D) will allow us to consider only cycles of length 2 when deriving the first-order asymptotics (in K) of solutions to the non-dimensionalized CME that is obtained from Eq. (20). While this last condition is not indispensable, it does allow for remarkable simplifications in the analysis.

In sum, the above set of conditions is certainly sufficient to ensure the applicability of the graph-based methodology developed in this article; however, we do not expect it to be optimal, or even minimal. We again refer the reader to Appendix C, where the verification of conditions (A) through (D) is sketched for two examples of reaction networks that involve enzyme catalysis.

Now, any given network generates a weighted graph G whose vertices represent all attainable states in the network, and which we label as in the definition of the matrix \mathbf{M} in Section 2.2; the weights of the edges in that graph correspond to the entries of its adjacency matrix \mathbf{M} . Thus, *e.g.*, the dimerization reaction discussed in detail in this article generates the graph shown in Fig. 4. (Entries on the diagonal of the matrix \mathbf{M} defined in (6) are omitted in that figure.)

6.1 Eigenvalue expansion

In our perturbation expansion for the eigenvalues of the transition state matrix \mathbf{M} in Section 2.4, we only employed algebraic considerations. The generalization of that expansion to potentially complex reaction processes will need to rely more heavily on concepts from graph theory [6]; recall Remark 3. In this subsection, we give a preliminary discussion, and we outline some potential challenges.

Because of condition (C), the constant terms in the expansion for each of the eigenvalues of \mathbf{M} are found on the diagonal of \mathbf{M}_0 ; these terms are obtained by imposing $K = 0$ and by noting that the determinant of a triangular matrix is the product of its diagonal entries. For $K > 0$, one can again associate the n -th eigenvalue λ_n of \mathbf{M} with the vertex labeled n . When calculating the determinant in (10) to determine the $O(K)$ term in the expansion for λ_n , only the permutations $\sigma_{n,n'} := (nn')$ with $n \sim n'$ and the identity will contribute, leading to the following generalized version of Eq. (11):

$$\begin{aligned} \det(\mathbf{M}_\lambda) &= \prod_{n \in V(G)} \{ \mathbf{M}_0[n, n] - a_0 + K(\mathbf{M}_1[n, n] - a_1) \} \\ &\quad - \sum_{\substack{n, n' \in V(G) \\ n' \sim n}} \mathbf{M}[n, n'] \mathbf{M}[n', n] \prod_{m \neq n, n'} (\mathbf{M}_0[m, m] - a_0). \end{aligned} \quad (21)$$

In sum, the first-order asymptotics (in K) of the n -th eigenvalue λ_n of \mathbf{M} can thus be obtained via the same reasoning as was applied in the derivation of Eq. (13). For simplicity, and without loss of generality, we restrict ourselves to the case where all eigenvalues of the “singular” transition matrix \mathbf{M}_0 are distinct:

Proposition 3. *Let conditions (A), (B), (C), and (D) be satisfied, and let G be the graph with adjacency matrix \mathbf{M} . Moreover, let all eigenvalues of \mathbf{M}_0 be of multiplicity one. Then,*

$$\lambda_n = \mathbf{M}_0[n, n] + K\mathbf{M}_1[n, n] - \sum_{n' \sim n} \frac{\mathbf{M}[n, n'] \mathbf{M}[n', n]}{\mathbf{M}_0[n', n'] - \mathbf{M}_0[n, n]} + o(K). \quad (22)$$

(We note that the third term in (22) is of order K , by condition (C), as well as that $\mathbf{M}_0[n', n'] \neq \mathbf{M}_0[n, n]$ for $n' \sim n$ and, hence, that the expansion in (22) is always well-defined; the proof is omitted here.)

Remark 12. Whenever two eigenvalues of $\mathbf{M} - \lambda_m$ and λ_n , say $-$ agree to leading order, the first product in Eq. (21) will not produce a term of order K , since $\mathbf{M}_0[m, m] - a_0^m = 0 = \mathbf{M}_0[n, n] - a_0^n$. Consequently, the system of (algebraic) equations in (21) which determines the asymptotics of these eigenvalues needs to be closed at higher order (in K) in that case, resulting in a generalised version of Eq. (22).

6.2 Eigenvector matrix

We shall impose conditions (A) through (D), as stated above; additionally, we again assume that all eigenvalues of \mathbf{M}_0 are distinct. By continuity, it then follows that the transition state matrix \mathbf{M} also has no multiple eigenvalues – at least when K is sufficiently small – which guarantees, in particular, that a non-zero column exists in the adjoint matrix of $\mathbf{M} - \lambda\mathbf{I}$; cf. Section 3.1. (In practice, one typically does not require K to be “too small.”)

Under these assumptions, we may extend the analysis of Section 3 to generalized reaction networks by applying again Proposition 1; hence, given some path \mathcal{P} in G , it remains to determine both the characteristic polynomial $Q(G \setminus \mathcal{P}, \lambda)$ and the weight $\omega(\mathcal{P})$ of \mathcal{P} .

To obtain an expression for $Q(G \setminus \mathcal{P}, \lambda)$, we essentially have to rederive Proposition 2 in this more general setting. To that end, we first need to generalize Definition 1: recalling that, under condition (C), each vertex $n \in V(G)$ of G corresponds uniquely to an eigenvalue λ_n of \mathbf{M} , we have

Definition 2. Let \mathcal{P} be a path in G , let $n \in V(G)$ such that $n \sim n'$ for some $n' \in \mathcal{P}$, and let λ_n be the eigenvalue corresponding to vertex n . Then, we define

$$\lambda_n^{\mathcal{P}} := \lambda_n + \sum_{\substack{n' \in \mathcal{P} \\ n' \sim n}} \frac{\mathbf{M}[n, n'] \mathbf{M}[n', n]}{\mathbf{M}_0[n', n'] - \mathbf{M}_0[n, n]}. \quad (23)$$

In other words, $\lambda_n^{\mathcal{P}}$ is equal to λ_n (up to first-order terms in K) minus all terms corresponding to permutations that exchange n with an index in \mathcal{P} . (We remark that these terms are negative, which implies the change in sign in (23), as compared to Eq. (22).)

In analogy to Proposition 2, we thus obtain

Proposition 4. *Let the conditions of Proposition 1 be satisfied, let \mathcal{P} be a path in G , and let $\mathcal{S}_{\mathcal{P}} := \{m' \in V(G) : m' \sim m, m \in \mathcal{P}\}$. (Here, we note that $\mathcal{P} \subseteq \mathcal{S}_{\mathcal{P}}$.) Then,*

$$Q(G \setminus \mathcal{P}, \lambda_n) = \prod_{m' \in \mathcal{S}_{\mathcal{P}} \setminus \mathcal{P}} (\lambda_{m'}^{\mathcal{P}} - \lambda_n) \prod_{m' \notin \mathcal{S}_{\mathcal{P}}} (\lambda_{m'} - \lambda_n) + o(K).$$

Remark 13. As was the case for the dimerization reaction discussed in Section 4, the eigenvalues of $G \setminus \mathcal{P}$ differ from the corresponding eigenvalues in G only due to permutations dropping out following the elimination of vertices associated with \mathcal{P} . Hence, for some values of n , the eigenvalue λ_n will have to be replaced with $\lambda_n^{\mathcal{P}}$ in the resulting characteristic polynomial.

Finally, the weight $\omega(\mathcal{P})$ of a given path \mathcal{P} depends on the topology of the graph G and must be determined on a case-by-case basis. Since chemical reaction networks typically result in very regular graphs, it is usually possible to obtain closed-form formulae for $\omega(\mathcal{P})$. Naturally, the more complex the network is, the more difficult it is to derive such formulae.

In sum, one thus finds the desired approximation for the matrix of eigenvectors \mathbf{E} that is associated with the transition state matrix \mathbf{M} . The inverse \mathbf{E}^{-1} of the matrix \mathbf{E} can be approximated in an analogous fashion, based on conditions (A) through (D); we omit the details here.

7 Conclusions and outlook

In the present article, we have solved the chemical master equation (CME), Eq. (5), which describes the dimerization reaction $A + A \xrightleftharpoons[k_2]{k_1} B$, by applying a novel graph-based approach to approximate the matrix of eigenvectors \mathbf{E} of the corresponding transition matrix \mathbf{M} , as well as the inverse \mathbf{E}^{-1} of that matrix; recall Eqs. (18) and (19). In Section 5, we have then compared our results with those obtained by direct matrix exponentiation, by the linear-noise approximation (LNA), and by the standard stochastic simulation algorithm (SSA) [16], and we have discussed strengths and weaknesses of our approach. Throughout, we have found the error incurred by our expansion for the probability distribution $\mathbf{P}(t)$ to be $O(K^2)$, which is consistent with a truncation at first order in K .

In particular, we have shown that our approach outperforms LNA for all times as long as the perturbation parameter K is sufficiently small; for larger values of K , there still exists some time interval – well away from steady state – during which LNA is inferior. However, if K is “too large,” our approximation predicts negative probabilities, which is indeed a general feature of perturbative techniques for approximating probability distribution functions [21]. Hence, admittedly, LNA performs reasonably well for “intermediate” values of both K and time t in the dimerization reaction considered here. However, we do not necessarily expect this conclusion to hold for more general reaction networks, in which our expansion may well remain consistent for larger K ; a precise characterization is left for future research [18, 20].

One could still ask oneself why it might not be preferable to evaluate the explicit solution for \mathbf{P} in (8) by direct matrix exponentiation. While the latter approach – which also involves the construction of the eigenvalue matrix Λ , as well as of the associated eigenvector matrices \mathbf{E} and \mathbf{E}^{-1} – is conceptually straightforward, preliminary numerical experiments suggest that both the involved computational effort and the execution time exceed those required by our graph-based methodology. Thus, for instance, taking $\Omega\alpha = 20$ and $K = 10^{-6}$, and setting the machine precision to 10^{-18} – which ensures that the error incurred by the two approaches is comparable – resulted in an execution time of less than half a second for our methodology, as compared to more than 6 seconds for matrix exponentiation, on an Intel Pentium® Dual-Core CPU T4500 running at 2.30 GHz with 3.00 GB of RAM, and averaged over 100 trials. However, our experiments relied on a brute-force implementation of matrix exponentiation that made use of built-in (“black-box”) routines provided by computer algebra packages such as MAPLE, which was used in the illustrative

example above. Hence, a more sophisticated (theoretical) analysis of the computational cost incurred by the two approaches is due before a definitive assessment can be made; see, *e.g.*, [32] and the references therein.

Alternatively, one could apply standard numerical integration techniques (such as Runge-Kutta) instead of matrix exponentiation to approximate the solution of the CME, Eq. (5), thus bypassing entirely the evaluation of the matrix product in (8) and reducing significantly the resulting computational effort. However, comparing the error incurred by the Fehlberg fourth-fifth-order Runge-Kutta method with degree four interpolant [9] against the solution calculated both by matrix exponentiation and via the graph-based approach developed in this article, we found that Runge-Kutta presents a markedly larger error during the initial (transient) phase, *i.e.*, before steady-state conditions set in. Again, further investigation – and, in particular, a systematic comparison with more advanced numerical techniques [33] – is required in order to assess authoritatively the accuracy provided by our methodology, as compared to these alternative approaches.

Finally, numerous “spectral” techniques have been suggested for the solution of the CME; for instance, Walczak *et al.* [36] studied reaction cascades by introducing generating functions which are then projected onto the eigenbasis of an appropriately defined “uncoupled” cascade. The projected equations can be solved, and the solution transformed back, to yield approximate joint probability distributions. Since that approach is not perturbative, unlike ours, it does not require the presence of a small parameter. However, it is assumed that there are no feedback “loops” in the cascade, the eigenbasis that is employed differs from ours, and the technique is applied to a generating function instead of to the CME itself. Hence, our methodology seems more general than theirs in some ways, yet more restrictive in others.

A definite advantage of the graph-based perturbation approach developed here lies in the fact that we have obtained an approximation for $\mathbf{P}(t)$ which is cheap to evaluate for varying values of the system parameters once the (non-dimensional) parameter $\Omega\alpha$ has been fixed. By contrast, any numerical solution of the CME can only give an approximation for fixed values of both $\Omega\alpha$ and K . Similarly, our approximation can easily be evaluated at any point in time, which allows us to avoid a time-step discretization and, hence, the resulting error that is necessarily incurred by numerical integration techniques. Compared with SSA, on the other hand, our approach benefits from the fact that it is not Monte-Carlo based, *i.e.*, that no repeated sampling is necessary to achieve the desired level of accuracy; rather, the quality of our approximation can be improved instantaneously simply by taking the parameter K to be sufficiently small.

Our graph-based approach has its own limitations, of course, two of which can be summarized as follows:

- (1) While we have found a suitable condition (“condition (D)” in Section 6) that allows us to avoid having to consider “too many” cycles in the calculation of the eigenvalues of the transition state matrix \mathbf{M} , we are still forced to account for all paths with constant weight when approximating the corresponding eigenvectors. (We cannot impose a condition to avoid such paths entirely, as chemical reaction networks always contain them.)
- (2) The evaluation of the product of the eigenvector matrix \mathbf{E} , the exponential of the eigenvalue matrix Λ , and the inverse \mathbf{E}^{-1} of \mathbf{E} – and, indeed, the normalization that is involved in approximating the matrix \mathbf{E}^{-1} itself, by Section 4.2 – can only be performed once $\Omega\alpha$ has been fixed, which implies that no closed-form formula is available for the probability distribution $\mathbf{P}(t)$ in Eq. (8).

To address the first point, we shall in the future investigate systematically the intrinsic structure of networks corresponding to chemical reaction processes; even so, the complexity involved in determining all possible paths between any two states in a network will realistically limit the applicability of our approach to small sets of reactions, as well as to those that exhibit additional structural properties. In order to tackle the second issue, we shall try to combine Proposition 1 with results obtained in [29], where a cofactor-dependent solution is found by application of the Laplace transform.

Another natural topic for future research concerns the question of how our approach can be extended to more general sets of chemical reactions. In Section 6, we have obtained some preliminary results in that direction; further investigation is required to identify suitable conditions on the associated graphs and, in particular, to improve on the conditions (A) through (D) imposed there. Thus, for instance, it might be feasible to omit condition (D) as long as any cycles of constant weight that occur in the graph associated with a given reaction process are “sufficiently short” and as long as the corresponding network structure is “reasonably regular;” recall Remark 11. The formulation of precise criteria is currently being investigated.

Appendix A Eigenvector formulae

In this appendix, we give complete formulae for the eigenvectors of the transition matrix \mathbf{M} for any value of $n = 0, 1, \dots, \Omega\alpha$, with $\Omega\alpha > 1$; in particular, we include the special cases where $n = 0, 1, \Omega\alpha$, which were omitted in Section 4.1. Then, we quote the corresponding (less compact) expressions that are obtained by retaining only asymptotically relevant terms, *i.e.*, terms up to and including $O(K)$, in these formulae. (We recall that, given an eigenvalue λ_n of \mathbf{M} , the n -th column $\mathbf{A}_n[i, n]$ of the adjoint matrix \mathbf{A}_n yields an associated eigenvector, which is then normalized to $\tilde{\mathbf{A}}_n[i, n]$; cf. again Section 4.1.)

$$\begin{array}{l}
 \boxed{1 < n < \Omega\alpha :} \\
 \tilde{\mathbf{A}}_n[i, n] = \begin{cases} -Kf(n)(\lambda_{n-2}^+ - \lambda_n)(\lambda_{n+1}^- - \lambda_n) \prod_{r=n+2}^{\Omega\alpha} (\lambda_r - \lambda_n) & \text{if } i = n - 1; \\
 (\lambda_{n-1}^+ - \lambda_n)(\lambda_{n+1}^- - \lambda_n)(\lambda_{n-2} - \lambda_n) \prod_{r=n+2}^{\Omega\alpha} (\lambda_r - \lambda_n) & \text{if } i = n; \\
 (-1)^{i-n}(\lambda_{n-1}^+ - \lambda_n)(\lambda_{i+1}^- - \lambda_n)(\lambda_{n-2} - \lambda_n) \prod_{r=i+2}^{\Omega\alpha} (\lambda_r - \lambda_n) \prod_{r=n}^{i-1} g(r) & \text{if } n < i < \Omega\alpha; \\
 o(K) & \text{otherwise.} \end{cases} \quad (24)
 \end{array}$$

$$\begin{array}{l}
 \boxed{n = 0 :} \\
 \tilde{\mathbf{A}}_n[i, 0] = \begin{cases} (\lambda_1^- - \lambda_0) \prod_{r=2}^{\Omega\alpha} (\lambda_r - \lambda_0) & \text{if } i = 0; \\
 (-1)^i(\lambda_{i+1}^- - \lambda_0) \prod_{r=i+2}^{\Omega\alpha} (\lambda_r - \lambda_0) \prod_{r=0}^{i-1} g(r) & \text{if } 0 < i < \Omega\alpha; \\
 o(K) & \text{otherwise.} \end{cases} \quad (25)
 \end{array}$$

$$\begin{array}{l}
 \boxed{n = 1 :} \\
 \tilde{\mathbf{A}}_n[i, 1] = \begin{cases} -2K(\lambda_2^- - \lambda_1) \prod_{r=3}^{\Omega\alpha} (\lambda_r - \lambda_1) & \text{if } i = 0; \\
 (\lambda_0^+ - \lambda_1)(\lambda_2^- - \lambda_1) \prod_{r=3}^{\Omega\alpha} (\lambda_r - \lambda_1) & \text{if } i = 1; \\
 (-1)^{i-1}(\lambda_0^+ - \lambda_1)(\lambda_{i+1}^- - \lambda_1) \prod_{r=i+2}^{\Omega\alpha} (\lambda_r - \lambda_1) & \text{if } 1 < i < \Omega\alpha; \\
 o(K) & \text{otherwise.} \end{cases} \quad (26)
 \end{array}$$

$$\begin{array}{l}
 \boxed{n = \Omega\alpha :} \\
 \tilde{\mathbf{A}}_n[i, \Omega\alpha] = \begin{cases} -Kf(\Omega\alpha)(\lambda_{\Omega\alpha-2}^+ - \lambda_{\Omega\alpha}) & \text{if } i = \Omega\alpha - 1; \\
 (\lambda_{\Omega\alpha-1}^+ - \lambda_{\Omega\alpha})(\lambda_{\Omega\alpha-2} - \lambda_{\Omega\alpha}) & \text{if } i = \Omega\alpha; \\
 o(K) & \text{otherwise.} \end{cases} \quad (27)
 \end{array}$$

Considering only the relevant terms in the above formulae, we find

$$\boxed{1 < n \leq \Omega\alpha :}
\tilde{\mathbf{A}}_n[i, n] = \begin{cases} 2Kf(n)(\Omega\alpha - n)! & \text{if } i = n - 1; \\ 2(\Omega\alpha - n)! \left\{ 1 - 2K \left[2(\Omega\alpha)^2 + (4n^2 - 6n + 6)\Omega\alpha - 4n^3 + 6n^2 - 15n + 10 \right] \right\} & \text{if } i = n; \\ (-1)^{i-n} \binom{\Omega\alpha - n}{\Omega\alpha - i} (\Omega\alpha - n)! \times \\ \left\{ 2 - K \left[8(\Omega\alpha)^2 + 4\Omega\alpha \left(2n^2 - 3n - 2i + 6 + \frac{n(2n-1)}{i-n+1} \right) \right. \right. \\ \left. \left. - 4 \left(2n^3 - n^2 - 2(i-8)n - 2i - 10 + \frac{n(2n-1)(n-1)}{i-n+1} \right) \right] \right\} & \text{if } i > n; \\ o(K) & \text{otherwise.} \end{cases} \quad (28)$$

$$\boxed{n = 0 :}
\tilde{\mathbf{A}}_n[i, 0] = \begin{cases} (\Omega\alpha)! - 4K\Omega\alpha(\Omega\alpha - 1)(\Omega\alpha)! & \text{if } i = 0; \\ (-1)^i \binom{\Omega\alpha}{\Omega\alpha - i} (\Omega\alpha)! \left[1 - 4K(\Omega\alpha - 1)(\Omega\alpha - i) \right] & \text{if } i > 0; \\ o(K) & \text{otherwise.} \end{cases} \quad (29)$$

$$\boxed{n = 1 :}
\tilde{\mathbf{A}}_n[i, 1] = \begin{cases} -2K(\Omega\alpha - 1)! & \text{if } i = 0; \\ -(\Omega\alpha - 1)! + 4K(\Omega\alpha - 1)(\Omega\alpha + 1)(\Omega\alpha - 1)! & \text{if } i = 1; \\ (-1)^i \binom{\Omega\alpha - 1}{\Omega\alpha - i} (\Omega\alpha - 1)! \left\{ 1 - K \left[4(\Omega\alpha)^2 - 4i\Omega\alpha + 2\frac{i+1}{i}\Omega\alpha + 8i - 12 \right] \right\} & \text{if } i > 1; \\ o(K) & \text{otherwise.} \end{cases} \quad (30)$$

Remark 14. We note that the particular case where $n = \Omega\alpha$, as given in Eq. (27), is contained in the more general Eq. (28), after simplification of the latter.

Similarly, we obtain the following formulae for the n -th row of the adjoint \mathbf{B}_n of $\mathbf{M}^T - \lambda_n \mathbf{I}$ introduced in Section 4.2 or, rather, for the normalized version $\tilde{\mathbf{B}}_n[n, i]$; here, we again assume $n = 0, 1, \dots, \Omega\alpha$, with $\Omega\alpha > 1$.

$$\boxed{1 \leq n < \Omega\alpha - 1 :}
\tilde{\mathbf{B}}_n[n, i] = \begin{cases} -Kf(n+1)(\lambda_{n-1}^+ - \lambda_n)(\lambda_{n+2}^- - \lambda_n) \prod_{r=0}^{n-2} (\lambda_r - \lambda_n) & \text{if } i = n + 1; \\ (\lambda_{n-1}^+ - \lambda_n)(\lambda_{n+1}^- - \lambda_n)(\lambda_{n+2}^- - \lambda_n) \prod_{r=0}^{n-2} (\lambda_r - \lambda_n) & \text{if } i = n; \\ (-1)^{n-i} (\lambda_{i-1}^+ - \lambda_n)(\lambda_{n+1}^- - \lambda_n)(\lambda_{n+2}^- - \lambda_n) \times \\ \prod_{r=0}^{i-2} (\lambda_r - \lambda_n) \prod_{r=i}^{n-1} g(r) & \text{if } 0 < i < n; \\ (-1)^n (\lambda_{n+1}^- - \lambda_n)(\lambda_{n+2}^- - \lambda_n) \prod_{r=i}^{n-1} g(r) & \text{if } i = 0; \\ o(K) & \text{otherwise.} \end{cases} \quad (31)$$

$$\boxed{n = 0 :}
\tilde{\mathbf{B}}_n[n, i] = \begin{cases} -2K(\lambda_2^- - \lambda_0) & \text{if } i = 1; \\ (\lambda_1^- - \lambda_0)(\lambda_2^- - \lambda_0) & \text{if } i = 0; \\ o(K) & \text{otherwise.} \end{cases} \quad (32)$$

$$\begin{aligned}
& \boxed{n = \Omega\alpha - 1 :} \\
\tilde{\mathbf{B}}_n[\Omega\alpha - 1, i] &= \begin{cases} -Kf(\Omega\alpha)(\lambda_{\Omega\alpha-2}^+ - \lambda_{\Omega\alpha-1}) \prod_{r=0}^{\Omega\alpha-3} (\lambda_r - \lambda_{\Omega\alpha-1}) & \text{if } i = \Omega\alpha; \\ (\lambda_{\Omega\alpha-2}^+ - \lambda_{\Omega\alpha-1})(\lambda_{\Omega\alpha}^- - \lambda_{\Omega\alpha-1}) \prod_{r=0}^{\Omega\alpha-3} (\lambda_r - \lambda_{\Omega\alpha-1}) & \text{if } i = \Omega\alpha - 1; \\ (-1)^{\Omega\alpha-1-i} (\lambda_{i-1}^+ - \lambda_{\Omega\alpha-1})(\lambda_{\Omega\alpha}^- - \lambda_{\Omega\alpha-1}) \times \\ \prod_{r=0}^{i-2} (\lambda_r - \lambda_{\Omega\alpha-1}) \prod_{r=i}^{\Omega\alpha-2} g(r) & \text{if } 0 < i < \Omega\alpha - 1; \\ (-1)^{\Omega\alpha-1} (\lambda_{\Omega\alpha}^- - \lambda_{\Omega\alpha-1}) \prod_{r=i}^{\Omega\alpha-2} g(r) & \text{if } i = 0; \\ o(K) & \text{otherwise.} \end{cases} \quad (33) \\
& \boxed{n = \Omega\alpha :} \\
\tilde{\mathbf{B}}_n[\Omega\alpha, i] &= 1. \quad (34)
\end{aligned}$$

In particular, the expression for $n = \Omega\alpha$ is obtained by observing that none of the remaining expressions for $\tilde{\mathbf{B}}_n[n, i]$ equals the vector $\mathbb{1}$ (or a multiple thereof). Hence, by Remark 8, we may take the last row to equal $\mathbb{1}$, after normalization.

In sum, considering only asymptotically relevant terms for $\Omega\alpha > 2$, we have

$$\begin{aligned}
& \boxed{0 \leq n < \Omega\alpha - 1 :} \\
\tilde{\mathbf{B}}_n[n, i] &= \begin{cases} 4K(-1)^{n-1}(2n+1)(n+1)! & \text{if } i = n+1; \\ (-1)^n n! \left\{ 2 - 4K[(4n^2 + 6n + 9)\Omega\alpha - (4n^3 + 6n^2 + 17n + 14)] \right\} & \text{if } i = n; \\ (-1)^{n-1} \frac{n!}{(n-i+1)!} \frac{(\Omega\alpha-i)!}{(\Omega\alpha-n)!} \left\{ 2(i-n-1) \right. \\ \left. + 4K \left[(2n^3 - (2i-5)n^2 + (i+12)n - 2i^2 - 6i + 9)\Omega\alpha - 2n^4 \right. \right. \\ \left. \left. + (2i-5)n^3 - (i+20)n^2 + (2i^2 + 14i - 31)n + 14(i-1) \right] \right\} & \text{if } 1 \leq i < n; \\ 2(-1)^n \frac{(\Omega\alpha)!}{(\Omega\alpha-n)!} \left\{ 1 - 2K[(2n^2 + 3n + 9)\Omega\alpha \right. \\ \left. - (2n^3 + 3n^2 + 17n + 14)] \right\} & \text{if } i = 0; \\ o(K) & \text{otherwise.} \end{cases} \quad (35)
\end{aligned}$$

$$\begin{aligned}
& \boxed{n = \Omega\alpha - 1 :} \\
\tilde{\mathbf{B}}_n[\Omega\alpha - 1, i] &= \begin{cases} 2K(-1)^{\Omega\alpha-2}(2\Omega\alpha-1)(\Omega\alpha)! & \text{if } i = \Omega\alpha; \\ (-1)^{\Omega\alpha-1}(\Omega\alpha-1)! [1 - 4K(2\Omega\alpha-1)(\Omega\alpha-1)] & \text{if } i = \Omega\alpha - 1; \\ (-1)^{\Omega\alpha-1}(\Omega\alpha-1)! \left\{ \Omega\alpha - i - 2K \left[2(\Omega\alpha)^3 \right. \right. \\ \left. \left. - (2i+5)(\Omega\alpha)^2 + 3(3i+1)\Omega\alpha - 2i(i+2) \right] \right\} & \text{if } 0 < i < \Omega\alpha - 1; \\ (-1)^{\Omega\alpha-1} (\lambda_{\Omega\alpha}^- - \lambda_{\Omega\alpha-1}) \prod_{r=i}^{\Omega\alpha-2} g(r) & \text{if } i = 0; \\ o(K) & \text{otherwise.} \end{cases} \quad (36) \\
& \boxed{n = \Omega\alpha :} \\
\tilde{\mathbf{B}}_n[\Omega\alpha, i] &= 1. \quad (37)
\end{aligned}$$

Remark 15. The particular case of $n = 0$ in Eq. (32) is contained in the more general Eq. (35); cf. also Remark 14 above.

Finally, we note that the restriction to $\Omega\alpha > 2$ is necessary to ensure that the products in Eq. (33) remain well-defined. When $\Omega\alpha = 2$, particular care has to be taken when evaluating the latter; still, one can show that, while $\tilde{\mathbf{B}}_1[1, 1] = -1 + 12K$ in that case, the above formulae for the remaining rows $\tilde{\mathbf{B}}_n[n, i]$ continue to be valid.

Appendix B Derivation of LNA

In Section 5.1, we compared the error incurred by LNA with the accuracy that is achieved by our perturbative approach. In this appendix, we present a concise derivation of LNA for the dimerization reaction on which our comparison was based.

Let $\phi(t)$ and $\psi(t)$ represent the concentrations of molecules of A and B , respectively, at time t . Then, the conventional rate equations [28] for the reaction scheme $A + A \xrightleftharpoons[k_2]{k_1} B$ are given by

$$\begin{aligned}\frac{d}{dt}\phi(t) &= -2k_1\phi(t)^2 + 2k_2\psi(t), \\ \frac{d}{dt}\psi(t) &= k_1\phi(t)^2 - k_2\psi(t).\end{aligned}$$

Assuming that $\phi(0) = 0$, *i.e.*, that the initial concentration of A is zero, we find

$$\phi(t) = \frac{4\alpha[e^{(c-1)t} - 1]}{c[e^{(c-1)t} + 1] - 2}, \quad (38)$$

$$\psi(t) = 2\alpha - \phi(t) \quad (39)$$

for the time-dependent solution of this pair of coupled differential equations, where

$$c := 1 + \sqrt{1 + 16\frac{k_1}{k_2}\alpha};$$

in particular, the conservation law in (39) implies $\psi(0) = 2\alpha$.

Now, the CME for the dimerization reaction, Eq. (2), can be rewritten as

$$\frac{d}{dt}\mathbb{P}(n_A, n_B, t) = \frac{k_1}{\Omega} [E_A^2 E_B^{-1} - 1] n_A (n_A - 1) \mathbb{P}(n_A, n_B, t) + k_2 [E_A^{-2} E_B - 1] n_B \mathbb{P}(n_A, n_B, t), \quad (40)$$

where $E_{n_j}^i$ is the step operator defined by

$$E_{n_j}^i f(n_1, n_2, \dots, n_j, \dots, n_d) = f(n_1, n_2, \dots, n_j + i, \dots, n_d).$$

The principal idea underlying LNA is to make the following change of variables [20] in (40):

$$n_A = \Omega\phi(t) + \Omega^{1/2}\xi(t) \quad \text{and} \quad n_B = \Omega\psi(t) + \Omega^{1/2}\eta(t).$$

(Typically, one assumes deterministic initial conditions, *i.e.*, one sets $\xi(0) = 0$ and $\eta(0) = 0$.) The above ansatz has the effect of transforming all functions of n_A and n_B into functions of the continuous random variables ξ and η , leading to a series expansion of Eq. (40) in powers of $\Omega^{1/2}$. The derivation is carried out for general chemical reaction networks in [20]; we simply quote the result here, as applied to dimerization:

$$\frac{\partial}{\partial t}\Pi = [4k_1\phi(t) + k_2] \frac{\partial}{\partial \xi}(\xi\Pi) + \frac{1}{2}[4k_1\phi(t) + 4k_2\alpha - 2k_2\phi(t)] \frac{\partial^2}{\partial \xi^2}\Pi + O(\Omega^{-1/2}), \quad (41)$$

where $\Pi := \Pi(\xi, t) := \mathbb{P}(n_A, t)$ denotes the reduced distribution, rewritten in terms of n_A only. (We note that we have also applied the conservation law from Eq. (39) in (41) to eliminate η , as $\xi + 2\eta = 0$, as well as that the above initial conditions correspond to assuming $\mathbb{P}(n_A = 0, t = 0) = 1$; recall Section 5.) The above equation is the Fokker-Planck

approximation to the CME; as its drift and diffusion coefficients are linear in ξ , it admits a Gaussian solution at all times.

Multiplying Eq. (41) by ξ and integrating, we find a differential equation for the mean $\langle \xi \rangle$,

$$\frac{d}{dt} \langle \xi \rangle = -[4k_1 \phi(t) + k_2] \langle \xi \rangle,$$

which, due to the deterministic initial condition $\xi(0) = 0$, implies $\langle \xi \rangle = 0$ for all times. Equivalently, we have

$$\langle n_A \rangle = \Omega \phi(t) + O(\Omega^{-1/2}) \quad \text{and} \quad \langle n_B \rangle = \Omega \psi(t) + O(\Omega^{-1/2}).$$

Hence, the mean concentrations obtained from LNA are identical to those obtained from the conventional rate equations.

The advantage of LNA lies in the resulting simple expression for the second moment $\langle \xi^2 \rangle$ of the distribution: multiplying Eq. (41) by ξ^2 and integrating with respect to ξ , we find the ordinary differential equation

$$\frac{d}{dt} \langle \xi^2 \rangle = -2[4k_1 \phi(t) + k_2] \langle \xi^2 \rangle + 4k_1 \phi(t)^2 + 2k_2 \psi(t),$$

which is known as the Lyapunov equation. In particular, the variance in the number of monomer molecules is then given by $\langle n_A^2 \rangle - \langle n_A \rangle^2 = \Omega(\langle \xi^2 \rangle - \langle \xi \rangle^2) = \Omega \langle \xi^2 \rangle$, which implies

$$p(x, t) = \frac{1}{\sqrt{2\pi\Omega\langle \xi^2 \rangle}} \exp \left[-\frac{1}{2} \left(\frac{x - \Omega\phi(t)}{\sqrt{\Omega\langle \xi^2 \rangle}} \right)^2 \right]$$

for the (continuous) probability density function that is obtained from LNA. Finally, to determine a corresponding discrete probability distribution for a given state n_A , we need to integrate p over a neighborhood of width 1 around that state:

$$\mathbb{P}(n_A, t) = \int_{n_A-1}^{n_A+1} p(x, t) dx. \quad (42)$$

Appendix C Additional examples

In this appendix, we present two additional examples to which the graph-based approach developed in this article can be applied. Given the motivational character of the following discussion, we omit much of the detail; rather, our intention is to show that conditions (A) through (D) imposed in Section 6 can be verified in a straightforward fashion.

C.1 Cooperative catalysis: case I

We first consider the catalytic mechanism that is described by [8]



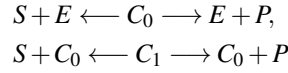
here, S , E , and P are substrate, (free) enzyme, and product, respectively, while C_0 and C_1 denote the two intermediate complexes.

As there is no input of molecules into the above network, condition (A) is trivially satisfied.

Next, dividing the CME that corresponds to the reaction scheme in (43) by k_2 , rescaling time, and abusing notation to denote the new non-dimensional time by t , as before, we obtain

$$\begin{aligned}
\frac{d}{dt} \mathbb{P}(n_S, n_E, n_{C_0}, n_{C_1}, n_P, t) = & K (E_S E_E E_{C_0}^{-1} - 1) n_S n_E \mathbb{P}(n_S, n_E, n_{C_0}, n_{C_1}, n_P, t) \\
& + (E_S^{-1} E_E^{-1} E_{C_0} - 1) n_{C_0} \mathbb{P}(n_S, n_E, n_{C_0}, n_{C_1}, n_P, t) \\
& + \frac{k_3}{k_2} (E_E^{-1} E_{C_0} E_P^{-1} - 1) n_{C_0} \mathbb{P}(n_S, n_E, n_{C_0}, n_{C_1}, n_P, t) \\
& + K \frac{k_4}{k_1} (E_S E_{C_0} E_{C_1}^{-1} - 1) n_S n_{C_0} \mathbb{P}(n_S, n_E, n_{C_0}, n_{C_1}, n_P, t) \\
& + \frac{k_5}{k_2} (E_S^{-1} E_{C_0}^{-1} E_{C_1} - 1) n_{C_1} \mathbb{P}(n_S, n_E, n_{C_0}, n_{C_1}, n_P, t) \\
& + \frac{k_6}{k_2} (E_{C_0}^{-1} E_{C_1} E_P^{-1} - 1) n_{C_1} \mathbb{P}(n_S, n_E, n_{C_0}, n_{C_1}, n_P, t)
\end{aligned} \tag{44}$$

for $K := \frac{k_1}{k_2 \Omega}$, where $E_{n_j}^i$ is the step operator defined in Appendix B. Thus, condition (B) holds in the limit as $K \rightarrow 0$. The “fast” transition matrix \mathbf{M}_0 , *i.e.*, the matrix corresponding to the “fast” subsystem



in the reaction scheme defined by (43), is lower triangular, since the associated graph is acyclic; hence, condition (C) is satisfied.

Finally, we need to show that condition (D) is met. Each reversible reaction in the scheme in (43) generates cycles of any even length $2d$ and weight $\Theta(K^d)$ (as long as they are compatible with the initial condition), since for each “fast” reaction, the reverse reaction is “slow,” and vice versa. Hence, the weight of cycles of length two is $\Theta(K)$, whereas it is $o(K)$ otherwise. It only remains to prove that there can be no other cycles, *i.e.*, cycles that involve one of the irreversible reactions. Now, each reaction R in the system is associated to a vector \mathbf{v}_R , which is given by the negative of the difference between a given state and the state of the system after R has occurred. Clearly, the corresponding reverse reaction $-R$ satisfies $\mathbf{v}_{-R} = -\mathbf{v}_R$. In our case, these vectors, arranged in columns in a stoichiometric matrix and excluding reverse reactions, are given by

$$\begin{pmatrix} 1 & 0 & 1 & 0 \\ 1 & 1 & 0 & 0 \\ -1 & -1 & 1 & 1 \\ 0 & 0 & -1 & -1 \\ 0 & 1 & 0 & 1 \end{pmatrix}. \tag{45}$$

(Here, the entries in each column correspond to the number of molecules of substrate, enzyme, complexes 0 and 1, and product, in that order.) A necessary condition for the existence of a cycle is for a linear combination of the columns of the above matrix to be zero. However, since the nullspace of (45) is generated by the vector $(1, -1, -1, 1)$, any such cycle would have to contain at least one of the reactions $P + E \longrightarrow C_0$ or $P + C_0 \longrightarrow C_1$; as neither of the two occurs in (43), we have verified (D).

Remark 16. We note that we implicitly assume $\frac{k_4}{k_1}$ to be constant as $K \rightarrow 0$ in (44), which imposes a direction in the parameter plane $(K, K \frac{k_4}{k_1})$. As that limit can be realised by fixing the rate constants in the reaction and by increasing the volume Ω , the direction taken is mathematically justified. (In practice, we require $k_1 \approx k_4$, $k_2 \approx k_3 \approx k_5 \approx k_6$, and $\Omega \gg \frac{k_1}{k_2}$.)

C.2 Cooperative catalysis: case II

In general, it may be necessary to study the reaction scheme in (43) in the limit as certain rate constants go either to zero or to infinity, thus specifying directions in the parameter space; one such limit, with $\frac{k_4}{k_1}$ constant, was studied in

the previous subsection. A potential further candidate that has been considered in the literature – albeit in the context of the derivation of the Hill equation via the deterministic rate equations – is defined by

$$\frac{k_2 + k_3}{k_1} \rightarrow \infty, \quad (46)$$

$$\frac{k_5 + k_6}{k_4} \rightarrow 0, \quad (47)$$

$$\frac{k_2 + k_3}{k_1} \frac{k_5 + k_6}{k_4} = K_m^2 \equiv \text{constant}, \quad (48)$$

as discussed for instance in [8]; here, $n_T = n + E + n_{C_0} + n_{C_1}$ denotes the total number of enzyme molecules that is present in the system.

We begin by noting that, obviously, condition (A) remains true, as shown in the previous subsection.

Next, we observe that the limits in Eqns. (46) and (47) can be achieved, for instance, if one assumes that k_2 and k_4 tend to infinity, while all other rate constants in the system and the reaction volume Ω remain fixed. (We remark that the left-hand sides in these equations correspond to the Michaelis-Menten constants for the first and second reactions in (43), respectively.) The direction thus imposed in Eq. (48) can then be written as

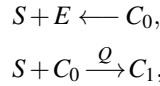
$$k_4 = \frac{k_5 + k_6}{K_m^2 k_1} (k_2 + k_3).$$

Dividing the CME corresponding to (43) by k_2 , rescaling time accordingly, and defining $K := \frac{1}{\Omega k_2}$, we obtain

$$\begin{aligned} \frac{d}{dt} \mathbb{P}(n_S, n_E, n_{C_0}, n_{C_1}, n_P, t) &= K (E_S E_E E_{C_0}^{-1} - 1) n_S n_E \mathbb{P}(n_S, n_E, n_{C_0}, n_{C_1}, n_P, t) \\ &+ (E_S^{-1} E_E^{-1} E_{C_0} - 1) n_{C_0} \mathbb{P}(n_S, n_E, n_{C_0}, n_{C_1}, n_P, t) \\ &+ \frac{\Omega k_3}{k_1} K (E_{C_0} E_E^{-1} E_P^{-1} - 1) n_{C_0} \mathbb{P}(n_S, n_E, n_{C_0}, n_{C_1}, n_P, t) \\ &+ \left(\frac{Q}{\Omega} + Q \frac{k_3}{k_1} K \right) (E_S E_{C_0} E_{C_1}^{-1} - 1) n_S n_{C_0} \mathbb{P}(n_S, n_E, n_{C_0}, n_{C_1}, n_P, t) \\ &+ \frac{\Omega k_5}{k_1} K (E_S^{-1} E_{C_0}^{-1} E_{C_1} - 1) n_{C_1} \mathbb{P}(n_S, n_E, n_{C_0}, n_{C_1}, n_P, t) \\ &+ \frac{\Omega k_6}{k_1} K (E_{C_1} E_{C_0}^{-1} E_P^{-1} - 1) n_{C_1} \mathbb{P}(n_S, n_E, n_{C_0}, n_{C_1}, n_P, t), \end{aligned}$$

where $Q := \frac{k_5 + k_6}{K_m^2 k_1}$ denotes a new parameter. Clearly, condition (B) is satisfied, since $K \rightarrow 0$ by definition.

To verify condition (C), we observe that the “fast” system

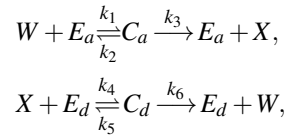


is acyclic. In fact, all states that are reachable from any fixed state \mathbf{n} are of the form $\mathbf{n} + \beta (1, 1, -1, 0, 0) + \gamma (-1, 0, -1, 1, 0)$, for some $\beta, \gamma \in \mathbb{N}$. Hence, no cycles can exist due to the linear independence of the vectors $(1, 1, -1, 0, 0)$ and $(-1, 0, -1, 1, 0)$.

Finally, it is easy to verify that condition (D) still holds, by the same argument as above.

C.3 Push-pull mechanism

As our second example, we consider the reaction scheme



which is known as the push-pull mechanism [34]. (Here, E_a and E_d denote free enzyme, with W and X the corresponding substrates and C_a and C_d the resulting complexes, respectively.) We study the parameter regime where $\frac{k_1}{\Omega}$ and $\frac{k_4}{\Omega}$ tend to infinity in such a manner that the ratio $k := \frac{k_1}{k_4}$ remains constant. Magnitudes of rate constants that are well-suited to that regime are common in prokaryotic and eukaryotic cells [1].

As usual, the validity of condition (A) is guaranteed by the absence of molecule input into the network.

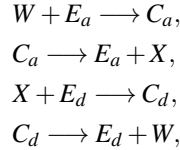
A non-dimensionalization that satisfies condition (C) is obtained by dividing the corresponding CME by $\frac{k_4}{\Omega}$, rescaling time, and by defining the small parameter $K := \Omega \frac{k_2}{k_4}$, which ensures that condition (B) is met. The resulting non-dimensional equation is given by

$$\begin{aligned} \frac{d}{dt} \mathbb{P}(n_W, n_{E_a}, n_{E_d}, n_{C_a}, n_{C_d}, n_X, t) &= k(E_W E_{E_a} E_{C_a}^{-1} - 1) n_W n_{E_a} \mathbb{P}(n_W, n_{E_a}, n_{E_d}, n_{C_a}, n_{C_d}, n_X, t) \\ &+ K(E_W^{-1} E_{E_a}^{-1} E_{C_a} - 1) n_{C_a} \mathbb{P}(n_W, n_{E_a}, n_{E_d}, n_{C_a}, n_{C_d}, n_X, t) \\ &+ \frac{k_3}{k_2} K(E_{E_a}^{-1} E_{C_a} E_X^{-1} - 1) n_{C_a} \mathbb{P}(n_W, n_{E_a}, n_{E_d}, n_{C_a}, n_{C_d}, n_X, t) \\ &+ (E_X E_{E_d} E_{C_d}^{-1} - 1) n_X n_{E_d} \mathbb{P}(n_W, n_{E_a}, n_{E_d}, n_{C_a}, n_{C_d}, n_X, t) \\ &+ \frac{k_5}{k_2} K(E_X^{-1} E_{E_a}^{-1} E_{C_d} - 1) n_{C_d} \mathbb{P}(n_W, n_{E_a}, n_{E_d}, n_{C_a}, n_{C_d}, n_X, t) \\ &+ \frac{k_6}{k_2} K(E_W E_{E_a} E_{C_a}^{-1} - 1) n_{C_d} \mathbb{P}(n_W, n_{E_a}, n_{E_d}, n_{C_a}, n_{C_d}, n_X, t). \end{aligned}$$

As in the previous example, the weight of cycles of length $2d$ that are generated by one of the reversible reactions in the above system is $\Theta(K^d)$. The associated stoichiometric matrix is given by

$$\begin{pmatrix} -1 & 0 & 0 & 1 \\ -1 & 1 & 0 & 0 \\ 0 & 0 & -1 & 1 \\ 1 & 1 & 0 & 0 \\ 0 & 0 & 1 & -1 \\ 0 & 1 & 1 & 0 \end{pmatrix};$$

its nullspace is spanned by the vector $(1, 1, 1, 1)$. The corresponding cycle is realized by the following set of reactions,



the weight of which is $\Theta(K^2)$. Other cycles could be obtained by permuting the above set; moreover, repeating each reaction in that set any given number of times in any order gives another cycle. Since, however, the weight of the resulting cycles is always $o(K)$, it follows that condition (D) is also satisfied.

References

- [1] S. B. van Albada and P. R. ten Wolde (2007), Enzyme localization can drastically affect signal amplification in signal transduction pathways, *PLoS Comput. Biol.* 3(10), e195.
- [2] B. Alberts, A. Johnson, J. Lewis, M. Raff, K. Roberts, and P. Walter (2007), *Molecular Biology of the Cell*, Garland Science, New York, NY, 5th edition.
- [3] H. Anton (1984), *Elementary Linear Algebra*, John Wiley & Sons, Hoboken, NJ, 4th edition.

- [4] M. Carchidi (1986), A method for finding the eigenvectors of an $n \times n$ matrix corresponding to eigenvalues of multiplicity one, *Amer. Math. Monthly* 93(8), 647–649.
- [5] T. M. Cover and J. A. Thomas (2006), *Elements of Information Theory* Wiley-Interscience [John Wiley & Sons], Hoboken, NJ, 2nd edition.
- [6] R. Diestel (2005), *Graph Theory*, Springer-Verlag, Berlin, 3rd edition.
- [7] J. Elf and M. Ehrenberg (2003), Fast evaluation of fluctuations in biochemical networks with the linear noise approximation, *Genome Res.* 13(11), 2475–2484.
- [8] C.P. Fall, E.S. Marland, and J.M. Wagner (2002), *Computational Cell Biology*, Springer-Verlag, New York.
- [9] E. Fehlberg (1970), Klassische Runge-Kutta-Formeln vierter und niedrigerer Ordnung mit Schrittweiten-Kontrolle und ihre Anwendung auf Wärmeleitungsprobleme, *Computing*, 6(1) 61–71.
- [10] L. Ferm, P. Lotstedt, and A. Hellander (2008), A hierarchy of approximations of the master equation scaled by a size parameter, *J. Sci. Comput.* 34(2), 127–151.
- [11] A. Fersht (1998), *Structure and Mechanism in Protein Science: A Guide to Enzyme Catalysis and Protein Folding*, W. H. Freeman, New York, NY, 1st edition.
- [12] C. Gadgil, C. H. Lee, and H. G. Othmer (2005), A stochastic analysis of first-order reaction networks, *B. Math. Biol.* 67(5), 901–946.
- [13] C.W. Gardiner (2009), *Handbook of stochastic methods for physics, chemistry and the natural sciences*, Springer-Verlag, Berlin, 4th edition.
- [14] C.W. Gardiner and S. Chaturvedi (1977), The poisson representation. I. A new technique for chemical master equations, *J. Stat. Phys.* 17(6), 429–468.
- [15] D. Gillespie (1992), A rigorous derivation of the chemical master equation, *Physica A* 188(1-3), 404–425.
- [16] D. Gillespie (2007), Stochastic simulation of chemical kinetics. *Ann. Rev. Phys. Chem.* 58(1), 35–55.
- [17] C. A. Gomez-Uribe and G. C. Verghese (2007), Mass fluctuation kinetics: Capturing stochastic effects in systems of chemical reactions through coupled mean-variance computations, *J. Chem. Phys.* 126(2), 024109.
- [18] R. Grima (2009), Noise-induced breakdown of the Michaelis-Menten equation in steady-state conditions, *Phys. Rev. Lett.* 102(21), 218103.
- [19] R. Grima (2010), Intrinsic biochemical noise in crowded intracellular conditions, *J. Chem. Phys.* 132, 185102.
- [20] R. Grima (2010), An effective rate equation approach to reaction kinetics in small volumes: Theory and application to biochemical reactions in nonequilibrium steady-state conditions, *J. Chem. Phys.* 133(3), 035101.
- [21] R. Grima (2011), Construction and accuracy of partial differential equation approximations to the chemical master equation, *Phys. Rev. E* 84(5), 056109.
- [22] R. Grima (2012), A study of the accuracy of moment-closure approximations for stochastic chemical kinetics, *J. Chem. Phys.* 136, 154105.
- [23] R. Grima, D. Schmidt, and T. J. Newman (2012), Steady-state fluctuations of a genetic feedback loop: an exact solution, *J. Chem. Phys.* 137, 035104.
- [24] R. Grima and S. Schnell (2008), Modelling reaction kinetics inside cells, *Essays Biochem.* 45(11), 41–56.
- [25] F. Hayot and C. Jayaprakash (2004), The linear noise approximation for molecular fluctuations within cells, *Phys. Biol.* 1(3-4), 205–210.

- [26] T. Jahnke and W. Huisinga (2007), Solving the chemical master equation for monomolecular reaction systems analytically, *J. Math. Biol.* 54(1), 1–26.
- [27] J. D. Klemm, S. L. Schreiber, and G. R. Crabtree (1998), Dimerization as a regulatory mechanism in signal transduction, *Annu. Rev. Immunol.* 16(1), 569–592.
- [28] E. Klipp, W. Liebermeister, C. Wierling, A. Kowald, H. Lehrach, and R. Herwig (2009), *Systems Biology: A Textbook*, Wiley-VCH Verlag, Weinheim, Germany, 1st edition.
- [29] I. J. Laurenzi (2000), An analytical solution of the stochastic master equation for reversible bimolecular reaction kinetics, *J. Chem. Phys.* 113(8), 3315–3322.
- [30] A. Mukherjee and K. Datta (1989), Two new graph-theoretical methods for generation of eigenvectors of chemical graphs, *J. Chem. Sci.* 101(6), 499–517.
- [31] B. Munsky and M. Khammash (2006), The finite state projection algorithm for the solution of the chemical master equation, *J. Chem. Phys.* 124(4), 044104.
- [32] V. Y. Pan, Z. Q. Chen, and A. Zheng (1998), The complexity of the algebraic eigenproblem, Technical Report 1998-071, Mathematical Sciences Research Institute, Berkeley, CA.
- [33] L. R. Petzold and U. M. Ascher (1998), *Computer Methods for Ordinary Differential Equations and Differential-Algebraic Equations*, Society for Industrial and Applied Mathematics, Philadelphia, PA, 1st edition.
- [34] S. Tănase-Nicola, P. B. Warren, and P. R. ten Wolde (2006), Signal detection, modularity, and the correlation between extrinsic and intrinsic noise in biochemical networks, *Phys. Rev. Lett.* 97(6), 068102.
- [35] N. G. van Kampen (2007), *Stochastic Processes in Physics and Chemistry*, North Holland, Amsterdam, The Netherlands, 3rd edition.
- [36] A. M. Walczak, A. Mugler, and C. H. Wiggins (2009), A stochastic spectral analysis of transcriptional regulatory cascades, *Proc. Natl. Acad. Sci. USA* 106(16), 6529–6534.